Article:

Amjad, M, Raza, G, Xin, Y et al. (4 more authors) (2017) Volumetric solar heating and steam generation via gold nanofluids. Applied Energy, 206. pp. 393-400. ISSN 0306-2619

https://doi.org/10.1016/j.apenergy.2017.08.144

Elsevier Editorial System(tm) for Applied Energy
Manuscript Draft

Manuscript Number: APEN-D-17-00899R1

Title: Volumetric solar heating and steam generation via gold nanofluids

Article Type: Research Paper

Keywords: Nanofluid, steam production, photothermal conversion, evaporation, direct absorption, solar energy

Corresponding Author: Professor Dongsheng Wen,

Corresponding Author's Institution: University of leeds

First Author: Muhammad Amjad

Order of Authors: Muhammad Amjad; Ghulam Raza; Yan Xin; Shahid Pervaiz; Jinliang Xu; Xiaoze Du; Dongsheng Wen

Abstract: Volumetric solar absorption using nanofluids can minimize the thermal loss by trapping the light inside the fluid volume. A strong surface boiling with the underneath fluid still subcooled could have many interesting applications, whose mechanism is however still under strong debate. This work advanced our understanding on volumetric fluid heating by performing a novel experiment under a unique uniform solar heating setup at 280 Suns, with a particular focus on the steam production phenomenon using gold nanofluids. To take the temperature distribution into account, a new integration method was used to calculate the sensible heating contribution. The results showed that the photothermal conversion efficiency was enhanced significantly by gold nanofluids. A three-stage heating scenario was identified and during the first stage, most of the energy was absorbed by the surface fluid, resulting in rapid vapor generation with the underneath fluid still subcooled. The condensed vapor analysis showed no nanoparticle escaping even under vigorous boiling conditions. Such results reveal that nanoparticle enabled volumetric solar heating could have many promising applications including clean water production in arid areas where abundant solar energy is available.

highlights

- Novel experiment was performed for nanofluids at a focused solar flux of 280 Suns.
- Strong surface evaporation was enabled while the bulk fluid was still subcooled
- A new integration method was used to calculate photothermal conversion efficiency
- Gold nanofluid (0.04w%) increased photothermal conversion efficiency by 95%.
- No nanoparticle was entrained with steam even under vigorous boiling

Graphical Abstract (for review)

Graphic abstract

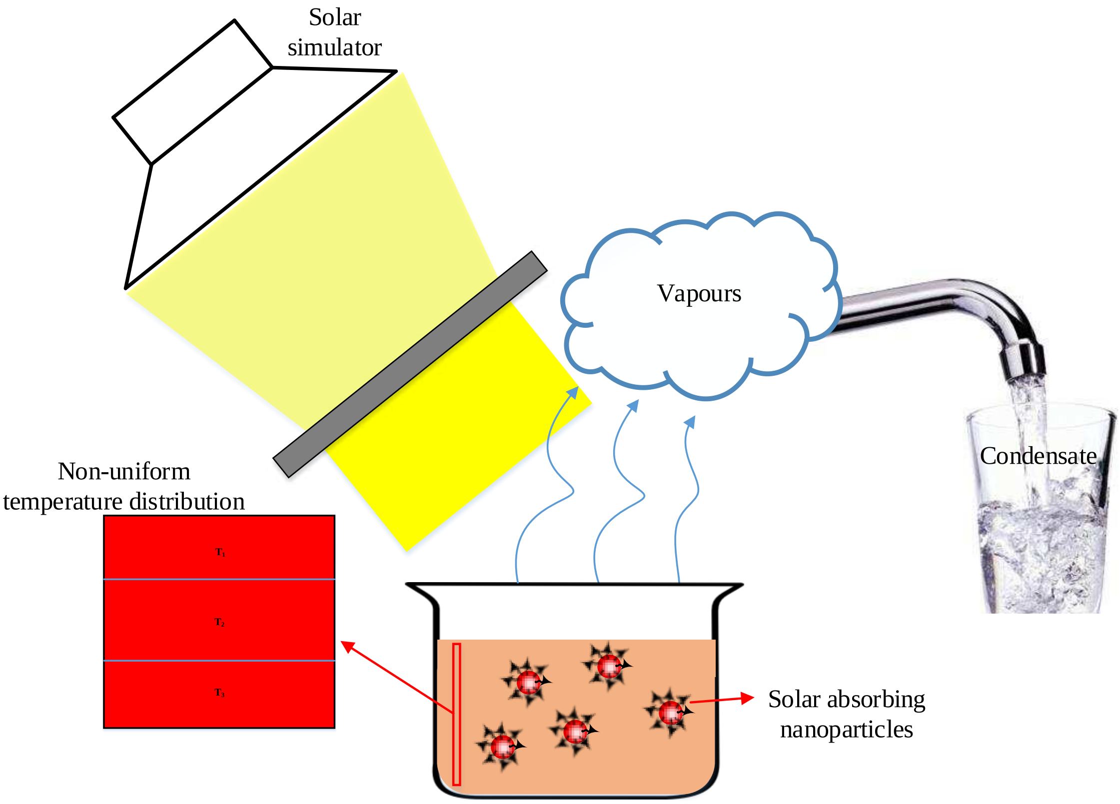

Reply to Reviewers' comments:

Manuscript Number: APEN-D-17-00899
Title: Volumetric solar heating and steam generation via gold nanofluids

---

The authors are grateful for all the constructive comments from the reviewer and the Editor. Most of the comments were concerned on the presentation of the work. We have addressed all these concerns in the revised version, and a point-by-point reply is supplied below

Reviewer #1:

The authors of the present work experimentally investigated the surface boiling and steam production mechanism of gold nanofluids under uniform solar heating of 280 Suns. Various concentrations of gold nanofluids were produced and the generated steam was condensed and tested to reveal the presence of any nanoparticles.

The study provides good insight to the surface boiling phenomenon of nanofluids and is in consonant with recent trend of investigation. However, there are several problems that need to be addressed before considering for publication in Applied Energy.

1. The Abstract, in its current state is incomplete. It is more like a conclusion and needs to be re-written.

   Action: the abstract was rewritten with more focus on the novelty

2. The use of "gold nanofluids" should be mentioned in the Title and Abstract.

   Action: The title was slightly changed to reflect the content, and the term “gold nanofluid” was used in the title and the abstract in the revised version.

3. In the statement: "For example, researchers [43] from Rice University", the Institution name should be replaced by the Authors' name.

Action: The authors’ name was used to replace the institution name in the revised version.

4. Section 2.2. line 37-38 must read: "Gold nanofluids were synthesized …", as we have one- and two- step "nanofluid" synthesis methods.

   Action: Modified as suggested.

5. In Fig. 2, the absorbance spectra of the gold nanofluids at 0.008, 0.016, 0.024 and 0.032 wt% are depicted. Fig. 5a shows the temperature vs. time plot of 0.040 wt %. For completion, the absorbance spectra of this concentration should also be measured and added to Fig. 2.

   Action: The absorbance of 0.040wt% of gold nanofluid is added in Fig. 2 in the revised version.

6. A photo of the experimental setup must be provided as well.

   Action: The photo of the experimental setup is updated with snaps of various components

7. In section 2.3., the thermal conductivity of the aerogel sheet insulation should be stated.

   Action: The thermal conductivity of the aerogel sheet is included in the revised version.

8. In section 2.3., the unit of the uncertainty of the digital weight balance should be given. (is it 0.001 gr or something else?)

   Action: This is gram (g) and is added in the revised version.

9. In section 3.1., it should be noted that Fig. 4 is for 0.016 wt% and Fig. 5 is for 0.040 wt% samples. (The legend of Fig.5a must read: "0.040 wt%")

   Action: The legend of Fig. 5a is updated in the revised version.

10. The distinction between the boiling characteristics of the two nanofluid samples and DI (Figs. 4-6) should be explicitly explained.

    Action: The suggestion is incorporated in the revised manuscript.

11. In section 3.1., the authors have stated: "As clearly seen from Fig. 5 (a) that the fluid temperature is not highly non-uniform,". Which one is correct? the fluid temperature is highly non-uniform or is not highly non-uniform??

    Action: The correct statement is “the fluid temperature is highly non-uniform”. This is corrected in the revised manuscript.

12. Since in section 3.1., first Fig. 7 is explained (mass of condensate vs. time) and afterwards efficiency (Figs 7-8) is illustrated, the text and formula regarding the absorbed energy (second page of 3.1. from line no. 10 to 55 and third page of 3.1. from line no. 1 to 29) should be inserted after the illustration of Fig. 7. (I wish you have provided page number for your manuscript!!)

    Action: The text and formulae have been displaced to the suggested location in the revised version.

13. How Eq. 3 was derived? any hint or reference?

Action: Eq. 3 was modified from the article by Jin et al. and the reference is given in the text in the revised manuscript.

14. Several typo errors exist throughout the manuscript. Third page of section 3.1. line 34, 39 and Fifth page of this section line 12: correct "nanolfuid". Third page of section 3.1. line 51 correct: "tendancy", Fourth page of section 3.1. line 25 correct: "volum" , Fifth page line 17 correct: "ehnaces"

    Action: The typos have been carefully corrected and the manuscript is proofread for any further typos of this type.

15. The relative uncertainty in the calculated photothermal efficiency should be provided within the illustration of Figs.8-9.

    Action: The relative uncertainty details are already given in supplementary information. We included the essential ones in the main text, and other information in the supplement.

16. Fourth page of section 3.1. lines 37-57 is a repetition of the above lines and should be briefed.

    Action: The repetition is removed and the text is briefed.

17. Fig. 8b is something totally different from Fig. 8a and should be inserted as an independent Figure. How the efficiency of sensible heating and steam generation in this figure were calculated?

    Action: Both Fig. 8a and Fig. 8b represents the radiation absorption efficiency and hence combined together. The sensible heating and steam generation efficiencies were calculated based on temperature rise and the amount of vapours generated over the time and given in Eq. (3). This is further elaborated in the revised version.

18. In section 3.2. , line 14 substituted "cooking" with "boiling" and also "left over" with "leftover" or another term such as "residue"

    Action: The substitution is done in the revised version as suggested.

19. Why the hydrodynamic size distribution of nanoparticles has maximum intensity at a smaller size after the experiments rather than a larger size? no agglomeration effects?

    Action: The maximum intensity of hydrodynamic size at a smaller size may be associated with the thinning of the stabilizer layer due to the treatment at higher temperatures. The residue sample after the experiment showed no agglomeration in the sample even if the thickness of the surfactant coating is reduced.

20. In section 3.2. line 44 delete: "ven"

    Action: Deleted.

21. Since the UV/Vis spectrum of the condensate and DI water of Fig. 10e are not completely overlapped, how can a potable water be ensured?

    Action: As there is no peak in the absorption spectrum of the condensate from gold nanofluid, it can be said that the gold nanoparticles are not escaped and the condensate is free of gold nanoparticles. A very small difference might be due to the dust of aerogel which is very light in weight and could be mixed with the vapours and finally condensed. This can be avoided by carefully selecting the insulation or handling the aerogel with high care to ensure the potable water quality.

22. In the first paragraph of the conclusion, explain "the effect of temperature distribution" on what?

    Action: “the effect of temperature distribution is on the photothermal conversion efficiency” and the same is corrected in text in revised manuscript.

23. Comparison should be made with related study to validate the claimed output. The manuscript would benefit from investigating the effect of varying solar flux and nanoparticle type.

    The study is related and compared with different relevant studies in the literature. Another investigation on various type of nanoparticles as suggested by the reviewer is in process and will be reported in the near future.

<u>Reviewer #2:</u>

a. The paper needs to be checked by a native language speaker for grammatical corrections.

    1. Page 13 line 34 spelling mistake "nanofluid"
    2. Page 13 line 39 spelling mistake of "concentration"
    3. Page 14 line 24 spelling mistake "volume"
    4. Page 14 line 54 spelling mistake "temperature"
    5. Page 15 line 6 please specify the concentration wt?? or v/v??
    6. Page 15 line 12 spelling mistake "nanofluid"
    7. Page 15 line 17 spelling mistake "enhances"
    8. Page 15 line 21 repetition of word. "of"
    9. Page 15 line 54 spelling mistake "evaporating"
    10. Page 16 line 14 spelling mistake.
    11. Page 16 line 37 spelling mistake.
    12. Page 16 line 44 spelling mistake.
    13. In highlights "wt" for percentage "t" is missing.

Action: A careful proof-reading was conducted, and many typos, including the above mentioned ones, are corrected in the revised version

b. In page 13 line 37-41, the authors reported" An enhancement of 80% for nanolfuid sample with concentration of 0.008 wt% and about 157% with concnetration of 0.040 wt% was observed over deionized water. And then in page 15 line 29-37, the authors reported " At a particle concentration of 0.040%, the overall photothermal efficiency or in a broader term the energy efficiency is enhanced by 95% over the base fluid in the experimental domain. This enhancement increases almost linearally with the nanoparticle concentration."

   Could the authors show a clear relationship between this behavior?

   Action: The statement “An enhancement of 80% for nanofluid sample with concentration of 0.008 wt% and about 157% with concentration of 0.040 wt% was observed over deionized water” is the enhancement in the vapour generation efficiency of gold nanofluid over the base fluid which is now clarified in the text to avoid confusion. The second statement “At a particle concentration of 0.040 wt%, the overall photothermal efficiency or in a broader term the energy efficiency is enhanced by 95% over the base fluid in the experimental domain. This enhancement increases almost linearly with the nanoparticle concentration” describes the overall photothermal conversion efficiency , which includes both the sensible heating efficiency and vapour generation efficiency. We have clarified these points in the revised version.

c. In fig. 2. The authors showed the absorbance of different volume fraction of nanoparticles but did not show 0.04%??

   Action: the absorbance spectrum of 0.040 wt% gold nanofluid sample is now included in Fig. 2 in the revised version.

d. In fig. 9 there is a different behavior between 0.008wt% and 0.016 wt%, can this be explained and why does this happen?

   Action: the behaviour between 0.008 wt% and 0.016 wt% is not different but the appearance was due to the nature of the curve i.e ‘spline’. The type of curve is changed to ‘straight’ in the revised version to avoid such confusion.

e. In fig. 10, e, can a better image be shown for comparison between DI and Au based DI??
   Action: The quality of Fig. 10 (e) is improved for a clear comparison between DI water and gold nanofluid.

From the Editors:

- An updated and complete literature review should be conducted. The relevance to Applied Energy should be enhanced with the considerations of scope and readership of the Journal.

We have provided updated references, including three papers from Applied Energy in the revised version

- A proof reading by a native English speaker should be conducted to improve both language and organization quality.

A carful proof reading was conducted, and many typos were corrected in the revised version. A tracking-change version is provided for reference.

- The originality of the paper needs to be further clarified. The present form does not have sufficient results to justify the novelty of a high quality journal paper.

The originality of the paper was further highlighted, as reflected in the Abstract, Introduction and Conclusion.

- The results should be further elaborated to show how they could be used for the real applications.

The application perspective was further elaborated in the revised version

*Revised Manuscript with No Changes Marked

Volumetric solar heating and steam generation via gold nanofluids

Muhammad Amjad[1, 4], Ghulam Raza[1], Yan Xin[3], Shahid Pervaiz[1], Jinliang Xu[3], Xiaoze Du[3], Dongsheng Wen [2,1*]

[1] School of Chemical and Process Engineering, University of Leeds, Leeds, LS2 9JT, UK

[2] School of Aeronautic Science and Engineering, Beihang University, Beijing, 100191, P.R. China

[3] School of Energy, Power and Mechanical Engineering, North China Electric University, Beijing 102206, P.R. China

[4] Department of Mechanical, Mechatronics and Manufacturing Engineering (KSK Campus), University of Engineering and Technology Lahore, Pakistan.

Abstract: Volumetric solar absorption using nanofluids can minimize the thermal loss by trapping the light inside the fluid volume. A strong surface boiling with the underneath fluid still subcooled could have many interesting applications, whose mechanism is however still under strong debate. This work advanced our understanding on volumetric fluid heating by performing a novel experiment under a unique uniform solar heating setup at 280 Suns, with a particular focus on the steam production phenomenon using gold nanofluids. To take the temperature distribution into account, a new integration method was used to calculate the sensible heating contribution. The results showed that the photothermal conversion efficiency was enhanced significantly by gold nanofluids. A three-stage heating scenario was identified and during the first stage, most of the energy was absorbed by the surface fluid, resulting in rapid vapor generation with the underneath fluid still subcooled. The condensed vapor analysis showed no nanoparticle escaping even under vigorous boiling conditions. Such results reveal that nanoparticle enabled volumetric solar heating could have many promising applications including clean water production in arid areas where abundant solar energy is available.

Keywords: Nanofluid, steam production, photothermal conversion, evaporation, direct absorption, solar energy

*Corresponding author. Tel.: 0044-113-3432678; fax: 0044-20-78825003.
Email address: d.wen@buaa.ac.uk / d.wen@leeds.edu.cn

1. Introduction

Solar energy is the most dominant renewable source that is available and accessible to everyone, but facing many challenges to achieve efficient utilization [1]. Wide-spread solar powered applications are not limited to but consist of electricity generation [2, 3], micro thermal power [4], chemical production line for methanol [5] and hydrogen [6], water desalination [7-10], greenhouse growth in agriculture [11], sterilization [12] and cooling and refrigeration [13, 14]. The solar energy utilization of these applications can be significantly enhanced by suspending various nano-sized particles in a fluid, which is called direct absorption volumetric solar collectors [15-19]. In contrast to conventional solar collectors [20, 21] where the solar absorption is surface-based, i.e., having large radiative and thermal losses due to high surface temperature[22], the volumetric solar collectors minimize these losses by thermal trapping [23, 24] and reduced temperature difference between the absorber and the fluid [25, 26].

A variety of direct absorption nanoparticles have been analyzed in terms of the enhancement in the photothermal performance, including Ag [27-29], Au [30-32], CNT (carbon nanotubes) [33-35], Cu [36], Al_2O_3 [37, 38], graphite [17], graphene [22], and TiO_2 [39]. In addition to the volumetric heating, direct vapor generation due to localized heating of nanoparticles [40-43] is a recent development in this area. For example, Neumann et al. [44] showed that by using very dilute gold nanoparticles (16.7 ppm) under a focused solar light via a typical Fresnel lens, steam was produced instantly while the measured bulk temperature was still 6 ^{o}C approximately. The calculated steam generation efficiency reached 80%, meaning only 20% of the solar radiation was used to increase the bulk fluid temperature. Later simulation work [44-46] showed the possibility of nanobubble formation based on a non-equilibrium phase change assumption. However these results are quite different to the recent results from Jin et al. [47]. Still using a

Fresnel lens (i.e. solar flux ~220 Suns), it revealed that steam generation was mainly caused by localized boiling and evaporation in superheated regimes due to a highly non-uniform temperature distribution, albeit the bulk fluid was still subcooled. The hypothesized nanobubble, i.e., steam produced around heated particles, was unlikely to occur under normal solar radiations. It shall be noted that all these experiments [44, 47, 48] were performed outdoor, where the solar flux varied from time to time, and the focus by Fresnel lens limited the heating to a small area, leading to a non-uniform solar energy input. Such would lead to a very high solar flux in localized areas, producing spot heating and high evaporation rate locally.

As far as the steam generation mechanism is concerned, it has been shown analytically that a minimum radiation flux of 3×10^8 W/m^2 is required to produce nanobubbles on heated nanoparticles [46, 49, 50], which can only be reached by powerful laser beams. In a separated study, Julien et al. [51] showed that 1×10^{10} W/m^2 was required to generate a nanobubble on a plasmonic gold nanoparticle. However quite differently, Hogan et al. [52] reported that ~ 1 MW/m^2 solar reflux was sufficient for efficient steam production due to a collective effect of nanoparticles that both scatter and absorb light, hence localizing light energy into mesoscale volumes.

It shall be noted that most of the experiments performed so far were not under well-controlled conditions [44, 47, 48]. Beside the problem of varying solar flux and spot heating mentioned above, most of the experiments were performed by a single-point temperature measurement, ignoring the temperature distribution in the bulk fluid [32, 44, 53]. Though Jin et al. [41] and Ni et al. [43] used multipoint temperature measurement, only the average temperature was used for the evaluation of the photothermal efficiency. In Jin's work [41], the spot heating and small fluid volume minimized the temperature stratification phenomenon, and the fluid reached saturated boiling rapidly , where the most interesting phenomenon under subcooled condition was insufficiently captured. In addition, possible escaping phenomenon of nanoparticles with the steam under saturated boiling has not been investigated, which is critical for any potential desalination or clean water production applications. Clearly a better understanding of the solar steam generation by nanoparticles is much needed.

This work aims to advance the field by answering three questions: i) Would the steam generation phenomenon be different under a uniform solar heating, instead of spot heating? ii) What is the underneath mechanism for steam production if not by forming nanobubbles? and iii) Would nanoparticle be escaped with the produced steam? To answer these questions, we performed a well-controlled experiment under a unique high power solar simulator (i.e. up to 4 MW/m^2) with a large focus area to provide uniform heating. A novel one-dimension test section was designed, and multiple thermocouples were used to reveal the temperature distribution along the heating path. A novel integration method was proposed to calculate the sensible heating contribution and to aid the analysis of steam production mechanism. Various concentrations of gold nanofluids were produced and used as the test fluids, and the generated steam was condensed to reveal the presence of any nanoparticles. All sample nanofluids before and after the experiments were carefully characterized in terms of stability, size distribution and morphological variation. Such would allow us to answer the proposed questions and advance the solar applications by direct absorption nanofluids.

2. Materials and methods

2.1. Reagents and devices

Hydrogen tetrachloroauric acid ($HAuCl_4$, Au ⩾ 49%) and Tri-sodium citrate ($Na_3C_6H_5O_7$, 99.8%) were purchased from Fisher Scientific and used as received. Deionized water was used throughout the experiments.

A transmission electron microscopy (TEM) (TECNAI, TF20) equipped with EDX (Energy Dispersive X-ray spectroscope), was used to analyze the morphology of the synthesized nanoparticles. The concentration of the gold dispersion was determined by an Atomic Absorption Spectrometer (AAS) (VARIAN, AA240FS). The hydrodynamic size and zeta potential of the nanofluids were obtained by a DLS (dynamic light scattering) device (Malvern nanosizer). The optical absorption of the nanofluid was examined by a UV/Vis spectrophotometer (HITACHI, U-3900) using a high precision cell with light path of 10mm.

2.2. Nanofluid synthesis and characterization

Gold nanoparticles (GNPs) were synthesized by the one-step method based on a modified thermal citrate reduction method as reported by Zhang at el. [32] and Chen et al. [54]. In the synthesis process, 100 ml of 5mM $HuACl_4$ solution was mixed with 100 ml of 10 mM trisodium citrate solution. The resultant mixture was heated to the boiling point until the mixture turned to wine red color. The resultant solution was continuously heated at 80 ^oC in a sonication bath for further 3 hours. Synthesized GNPs were aged at room temperature for 24 hours and cleaned by dialysis from 8 kDa membrane. The membrane allows the excessive ions to diffuse smoothly from the suspension and blocks the GNPs. DI water was changed twice a day for a period of 10 days, leading to pure GNPs dispersions. The concentration of the resulting nanofluid was measured by Atomic Absorption Spectrometry (AAS).

The morphology of the synthesized nanoparticles was analyzed by a TEM and the hydrodynamic size was measured by the DLS device. **Fig 1 (a)** shows the TEM image of the nanoparticles and the inset shows a close view. It can be seen that the gold nanoparticles are mostly spherical with particle size in the range of 20~ 30 nm. The hydrodynamic size distribution of the gold particles, **Fig. 1 (b)**, shows a slightly larger size than that from TEM, which is due to the hydrodynamic nature of size measurement by DLS.

The optical absorbance of Au nanofluids was checked by UV/Vis spectrophotometer (U-3900, HITACHI) using a high precision cell with light path of 10 mm. The absorbance is defined as the logarithm (10 as base) of reciprocal of transmittance, whereas the transmittance is the ratio of the transmitted light by the nanofluid sample to the incident light. According to the Beer-Lambert's Law [53], absorbance is $log\ (I_o/I) = \epsilon lc$, where I_o is the incident light on the sample, I is the light transmitted, ϵ is the extinction coefficient, l is the length of the sample through which light passed, and c is the concentration of the nanofluid. The absorbance of Au nanofluid is shown in **Fig.2**, where the inset shows a linear relationship of the absorbance peak with the concentration. The absorbance peak of the Au nanofluid appears at a wavelength of 525 nm and is identical for various concentrations. The absorbance peak can be engineered and shifted towards longer wavelength by controlling the size and shape of the nanoparticles during the synthesis process.

2.3. Experimental setup

Photothermal conversion characteristics and steam generation capability of the characterized gold nanofluids were investigated using a solar simulator having seven xenon short-arc lamps aligned on the reflector ellipsoidal axis [55]. The solar simulator is capable of producing a concentrated solar flux of about 4 MW/m^2 when all of seven lamps are in operation, for more details about the solar simulator, please refer to **Section I of the supplementary information**.

Only one lamp was put in operation for the current experiments to deliver a solar flux equivalent to 280 Suns. The solar radiation had a focal area of 28.27 cm^2, which was passed through a custom-made aperture (30 mm diameter) of aerogel sheet wrapped in aluminum foil. The test section was made of high temperature quartz glass with the inner and outer diameter of 30 mm and 34 mm respectively. The test section was put accurately under the solar radiator to enable a uniform heating. A sample fluid of 25 ml (~35.4 mm depth) was filled into and covered with a transparent quartz cover. Holes of 1 mm diameter were fabricated in the vessel to insert the thermocouples equidistant to each other at 10 mm. The vessel was covered with a tightly packed aerogel blanket with thermal conductivity of 0.015W/m^2K to minimize the heat loss to the surroundings. A square glass box was used to contain the aerogel with the vessel fitted in a hole in the aerogel sheets, and further details can be seen in **Section II of the supplementary information**.

Three K-type (Omega 5TC-TT-K-36-36) thermocouples (TC) were used to measure the bulk fluid temperature, positioned evenly along the optical depth in top, middle and bottom sections of the sample fluid at distance of 10 mm from each other. This was to ensure that neither the top TC was exposed to the air during the experiment nor the bottom TC touched the bottom of the vessel. The temperature of the vapor generated was measured through an additional K-type thermocouple. The steam temperature was measured at the middle of a 20 mm long exit channel, as shown in **Fig. 3**. The temperature was registered by a data logger (Agilent 34970A) linked to a computer. The uncertainty in temperature measurement was validated as ±0.25 K. The generated steam was condensed in a glass condenser with cooling water circulating around the condensing tube. A sensitive digital balance (Setra, BL-500S) with uncertainty of ±0.001g was used to measure the mass of the condensed vapor.

3. Results and discussion

3.1. Fluid heating and steam characterization

The bulk fluid temperature was measured by three thermocouples TC1, TC2 and TC3 as the nanofluid sample was heated under a solar flux of 280 Suns. The top TC1 showed a rapid change in fluid temperature as the sample is illuminated. Depending upon the variation of bulk fluid temperature, **Fig.4,** the fluid heating can be divided into three phases. The first phase is the heating of surface fluid with the underneath fluid in subcooled condition. The surface fluid reaches to the boiling temperature rapidly and the temperature of the underneath layers of the fluid volume is slightly changed **(Fig. 4 and Fig. 5).** The second phase is the heating of bulk fluid volume in which the heat flux penetrates and brings the temperature of the whole fluid volume to the boiling point. The third phase is the saturated boiling phase in which the sample volume temperature reaches the boiling point. Due to the superheating, the steam temperature continues to increase above the boiling temperature until the radiation flux is switched off. The temperature distribution in the first two heating phases can be clearly seen in **Fig. 5 (a),** in which the concentration of gold nanoparticles is 0.04 wt%. The non-uniformity of temperature along the heating path is increased with the increase of nanoparticle concentration. This is associated with the increased radiation absorption at the surface due to more solar energy trapping at the surface at a higher concentration. The temperature distribution for deionized water sample is shown in **Fig. 6** as a comparison, and more non-uniform temperature profile can be referred to **Section III of the supplementary information.** It is evident from Fig. 6 that for DI water, there is not much temperature variation along the heating path during the initial volumetric heating phase. The rate of rise in surface temperature is also much slower than that of 0.040 wt% gold nanofluid **(Fig. 5a)**

Although the thermophysical properties of water like thermal conductivity and specific heat capacity would be changed with the addition of nanoparticles. However with such a small nanoparticle concentration (0.040 wt%), the change in these properties was found to be negligible. The mass of the condensed vapor generated over a 5-min duration is given in **Fig. 7**, which shows a siginificanlty higher value for nanofluid samples . Comparing with DI water, an enhancement of 80% and 157% in the vapor generation efficiency are observed for gold nanofluids at 0.008 wt% and 0.040 wt% respectively. The amount of condensed vapor is increased nearly linearly with the increase of nanoparticle concentration, as presented in **Fig.7** (inset). The variation in the mass of condensate at the initital volumetric heating of the samples with varying concentration is small, which might be due to the recondensation of the vapors. The vapors generated under subcooled conditions have greater tendency of recondensation due to the presene of cold vessel walls. A constant evaporation rate after the phase two of the volumetric heating confirms the saturated boiling in the nanofluid sample. The uncertainty in the mass measurement for the sample with 0.008 wt% nanoparticle concentration was estimated to be ±0.592% for the first 60 seconds of illumination. The relative uncertianty in the calculated photothermal efficiency was estimated to be ±2%, and detailed uncertainty analyiss can be found in the **Section IV of the supplementary information**

The energy absorbed by the nanofluid during the sensible heating period was calculated using the following relation by Zhang et al. [32, 53] and Neumann [44], where only one temperature sensor was used to represent the bulk fluid temperature;

$$Q = c_p m \Delta T \qquad (1)$$

where c_p, m and ΔT are the specific heat capacity, mass of the sample taken and temperature change of the fluid volume over the specified time. The change in temperature ΔT was replaced by $\Delta\bar{T}$, i.e., the average temperature difference by Jin et al. [41, 48], in which more than one thermocouple were used. As clearly seen from **Fig. 5 (a)** that the fluid temperature is highly non-uniform, the temperature measured by only one thermocouple is clearly not representing the fluid temperature. The calculated absorbed energy may be overestimated or under-estimated depending upon the position of the thermocouple. Even the average value of the temperature may also be misleading depending upon several factors, including the type of nanoparticles, their concentrations, color of the nanofluid and intensity of radiation flux.

Here we use a more realistic method to calculate the energy absorbed by the nanofluid volume. The fluid volume is divided into various temperature dependent sections as shown in **Fig. 5(b)**. The absorbed energy of the each section is calculated independently and the overall absorbed energy is evaluated using the relation given in Eq. 2;

$$Q = c_p \sum_{i=1}^{n} (m_i \Delta T_i) \qquad (2)$$

. The overall photothermal conversion efficiency (η_{PTC}) including sensible heating and latent heat is subsequently calculated from Eq. 3, which is a modified version of the equation used by Jin et al. [41];

$$\eta_{PTC} = \frac{c_p \sum_{i=1}^{n} (m_i \Delta T_i) + \int_0^t L_v m_v dt}{\int_0^t I A_a dt} \qquad (3)$$

where I is the solar irradiance, A_a is the area of the aperture, L_v is the latent heat of vaporization of water and m_v is mass of the condensed vapors in time dt.

Fig 8 (a) shows the photothermal conversion efficiency during the first phase, i.e. surface heating which is typically less than 30 seconds after the heating. The efficiency includes the sensible and latent heat contributions. As can be observed in **Fig 8 (a)** that the position of the thermocouple has a great influence in determining the photothermal efficiency. If only one thermocouple is used for the measurement of temperature change as in [32, 44, 53] and the optical length of the fluid volume is significant, the obtained photothermal efficiency would be underestimated if the thermocouple is away from the surface (as TC3 here in this study) and overestimated (as TC1 in this study) if it is close to the surface. This underestimation or overestimation is because the temperature of the respective thermocouple is used to represent the temperature of the whole fluid volume at any instant, but actually it is not as already shown in **Fig. 5 (a)**. Using the proposed method of calculating the photothermal efficiency, i.e. taking the temperature distribution into account, gives more realiable results and is necessacitated particulary when the temperature remains below the boiling temperaure of the nanofluid.

Fig 8 (b) shows in the efficiency of sensible heating and steam generation in the proposed three phases (**Fig. 4**) during the irradiance time of 5 min for a nanoparticle concentration of 0.040 wt%. During the surface heating, most of the absorbed energy is used in the sensible heating of the nanofluid, together with some vapor generated.while in case of DI water, no vapor were observed in the surface heating phase. Hence the presence of nanoparticles enhances the steam genergation efficiency even under subcooled condition as also observed by Jin et al. [41]. The steam generation efficiency of about 95% in the saturated boiling is very attractive and gives an enhancement of 117.5% over the base fluid.

Fig. 9 shows the overall efficiency of the plasmonic gold nanofluid at various concentrations compared to the base fluid. The photothermal efficiency is dramatically enhanced by gold nanoparticles . At a particle concentration of 0.040 wt%, the overall photothermal efficiency or in a broader term the energy efficiency is enhanced by 95% over the base fluid in the experimental domain. This enhancement increases almost linearaly with the nanoparticle concentration. It can also be noticed that the efficiency difference among the three modes of its evaluation is negligibly small when there is no nanoparticle in the base fluid. But with the addition and increase in the concentation of the nanoparticles, this difference is magnified. This is due to the non-uniform temperature distribution (**Fig. 4**) caused by the presence of the nanoparticles. This non-uniform temperature distrbution is very supportive in evaporating the fluid from the surface while keeping the bulk volume under subcooled conditions. This phenomenon can be used to produce clean water by evaporating the water from the surface and keep circulating the underneath volume like in forward osmosis desalination.

3.2. Analysis of nanoparticles after experiments

The remaining concentrated nanosuspension after the experiments was examined in terms of stability, nanoparticle size distribution and morphological appearance it had undergone. **Fig 10 (a)** and **(b)** represents the TEM micrograph and hydrodynamic size distribution of the particles after boiling repectively. Compared with the characterization results before the experiment, the size and shape of the gold nanoparticles is almost the same after the experiment. The hydrodynamic size distribution of the nanoparticle is slightly changed and has a maximum intensity at 44 nm, which was at 49 nm before the experiments. The size inensity distribution is more compact and peaked after the photothermal coversion experiments. An additional smaller peak is observed in the DLS size distribution. This might be due to the collapse of the surfactant layer on the surface of the nanoparticles. The zeta potential of the nanofluid after the steam generation experiement is about -37 mV as shown in in Fig. **10 (d)**, which indicates a good stability of the suspension.

As to the possible nanoparticle entrainment phenomenon, **Fig. 10 (c)** shows that the remaining concentrated gold nanofluid in dark red wine color and the condensate in transparent. The UV/Vis spectrum of the condensate presented in **Fig 10 (e)** also confirms that no particles were blown out with the steam even under strong boiling conditions. This phenomon is very helpful for solar desalination applications, where potable water could be produced following vapor generation, induced by highly absorptive nanopaticles.

4. Conclusion

A well-controlled steam generation experiment was performed by using gold nanofluids under a concentrated solar flux of 280 Suns, and the main conclusions can be summarized:

- Highly non-uniform temperature distribution was found t along the heating path of gold nanofluids and an integration method was proposed to calculate the sensible heating contribution.
- Three phases of heating was identified, i.e., surface heating, subcooled boiling and saturated boiling. During the surface heating phase, most of the energy was absorbed by the surface fluid, resulting in vapor generation while the underneath fluid still subcooled. .
- The photothermal conversion efficiency and steam generation performance increased almost linearly with the increase of particle concentration. An enhancement in the energy efficiency of about 95% over the base fluid was achieved for 0.04 wt% gold nanofluids.
- The analysis of the condensed vapor proved the absence of gold nanoparticle, suggesting that the nanoparticles were not entrained by the vapor even under vigorous boiling.

Acknowledgement

The authors acknowledge the support from University of Engineering and Technology Lahore in collaboration with Higher Education Commission of Pakistan under Faculty Development Program, the National Science Foundation of China (Grant No. 51228601) and British Council Newton Fund-PhD Placement Grant (Grant No. 473117) for this work.

References

1. Modi, A., et al., *A review of solar energy based heat and power generation systems.* Renewable and Sustainable Energy Reviews, 2017. **67**: p. 1047-1064.
2. Manente, G., *High performance integrated solar combined cycles with minimum modifications to the combined cycle power plant design.* Energy Conversion and Management, 2016. **111**: p. 186-197.
3. Gupta, M.K. and S.C. Kaushik, *Exergy analysis and investigation for various feed water heaters of direct steam generation solar–thermal power plant.* Renewable Energy, 2010. **35**(6): p. 1228-1235.
4. Maghanki, M.M., et al., *Micro combined heat and power (MCHP) technologies and applications.* Renewable and Sustainable Energy Reviews, 2013. **28**: p. 510-524.
5. Bai, Z., et al., *A polygeneration system for the methanol production and the power generation with the solar–biomass thermal gasification.* Energy Conversion and Management, 2015. **102**: p. 190-201.
6. Ozturk, M. and I. Dincer, *Thermodynamic analysis of a solar-based multi-generation system with hydrogen production.* Applied Thermal Engineering, 2013. **51**(1–2): p. 1235-1244.
7. Tiwari, G.N., H.N. Singh, and R. Tripathi, *Present status of solar distillation.* Solar Energy, 2003. **75**(5): p. 367-373.
8. Ali, M.T., H.E.S. Fath, and P.R. Armstrong, *A comprehensive techno-economical review of indirect solar desalination.* Renewable and Sustainable Energy Reviews, 2011. **15**(8): p. 4187-4199.
9. Gude, V.G., N. Nirmalakhandan, and S. Deng, *Desalination using solar energy: Towards sustainability.* Energy, 2011. **36**(1): p. 78-85.
10. Shannon, M.A., *Water desalination: Fresh for less.* Nat Nano, 2010. **5**(4): p. 248-250.
11. Hassanien, R.H.E., M. Li, and W. Dong Lin, *Advanced applications of solar energy in agricultural greenhouses.* Renewable and Sustainable Energy Reviews, 2016. **54**: p. 989-1001.
12. Dravid, M.N., et al., *The use of solar energy for powering a portable autoclave.* Journal of Hospital Infection, 2012. **80**(4): p. 345-347.
13. Modi, A., et al., *Performance analysis of a solar photovoltaic operated domestic refrigerator.* Applied Energy, 2009. **86**(12): p. 2583-2591.
14. Ullah, K.R., et al., *A review of solar thermal refrigeration and cooling methods.* Renewable and Sustainable Energy Reviews, 2013. **24**: p. 499-513.
15. Govorov, A.O. and H.H. Richardson, *Generating heat with metal nanoparticles.* Nano Today, 2007. **2**(1): p. 30-38.
16. Menbari, A., A.A. Alemrajabi, and A. Rezaei, *Heat transfer analysis and the effect of CuO/Water nanofluid on direct absorption concentrating solar collector.* Applied Thermal Engineering, 2016. **104**: p. 176-183.

17. Otanicar, T.P., et al., *Nanofluid-based direct absorption solar collector.* Journal of Renewable and Sustainable Energy, 2010. **2**(3): p. 033102.
18. Parvin, S., R. Nasrin, and M.A. Alim, *Heat transfer and entropy generation through nanofluid filled direct absorption solar collector.* International Journal of Heat and Mass Transfer, 2014. **71**: p. 386-395.
19. Vijayaraghavan, S., S. Ganapathisubbu, and C. Santosh Kumar, *Performance analysis of a spectrally selective concentrating direct absorption collector.* Solar Energy, 2013. **97**: p. 418-425.
20. Tian, Y. and C.Y. Zhao, *A review of solar collectors and thermal energy storage in solar thermal applications.* Applied Energy, 2013. **104**: p. 538-553.
21. Kalogirou, S.A., *Solar thermal collectors and applications.* Progress in Energy and Combustion Science, 2004. **30**(3): p. 231-295.
22. Liu, J., et al., *A combined numerical and experimental study on graphene/ionic liquid nanofluid based direct absorption solar collector.* Solar Energy Materials and Solar Cells, 2015. **136**: p. 177-186.
23. Wijeysundera, N.E. and V. Thevendran, *A two-dimensional heat transfer analysis of the thermal-trap collector.* Solar Energy, 1988. **40**(2): p. 127-133.
24. Arai, N., Y. Itaya, and M. Hasatani, *Development of a "volume heat-trap" type solar collector using a fine-particle semitransparent liquid suspension (FPSS) as a heat vehicle and heat storage medium Unsteady, one-dimensional heat transfer in a horizontal FPSS layer heated by thermal radiation.* Solar Energy, 1984. **32**(1): p. 49-56.
25. Boriskina, S.V., H. Ghasemi, and G. Chen, *Plasmonic materials for energy: From physics to applications.* Materials Today, 2013. **16**(10): p. 375-386.
26. Lenert, A. and E.N. Wang, *Optimization of nanofluid volumetric receivers for solar thermal energy conversion.* Solar Energy, 2012. **86**(1): p. 253-265.
27. Chen, M., et al., *An experimental investigation on sunlight absorption characteristics of silver nanofluids.* Solar Energy, 2015. **115**: p. 85-94.
28. Bandarra Filho, E.P., et al., *Experimental investigation of a silver nanoparticle-based direct absorption solar thermal system.* Energy Conversion and Management, 2014. **84**: p. 261-267.
29. Chen, M., et al., *Investigating the collector efficiency of silver nanofluids based direct absorption solar collectors.* Applied Energy, 2016. **181**: p. 65-74.
30. Eustis, S. and M.A. El-Sayed, *Why gold nanoparticles are more precious than pretty gold: Noble metal surface plasmon resonance and its enhancement of the radiative and nonradiative properties of nanocrystals of different shapes.* Chemical Society Reviews, 2006. **35**(3): p. 209-217.
31. Pérez-Juste, J., et al., *Gold nanorods: Synthesis, characterization and applications.* Coordination Chemistry Reviews, 2005. **249**(17–18): p. 1870-1901.
32. Zhang, H., et al., *Photothermal conversion characteristics of gold nanoparticle dispersions.* Solar Energy, 2014. **100**: p. 141-147.
33. Rahman, M.M., et al., *Effect of solid volume fraction and tilt angle in a quarter circular solar thermal collectors filled with CNT–water nanofluid.* International Communications in Heat and Mass Transfer, 2014. **57**: p. 79-90.
34. Said, Z., et al., *Analyses of exergy efficiency and pumping power for a conventional flat plate solar collector using SWCNTs based nanofluid.* Energy and Buildings, 2014. **78**: p. 1-9.
35. Yousefi, T., et al., *An experimental investigation on the effect of pH variation of MWCNT–H2O nanofluid on the efficiency of a flat-plate solar collector.* Solar Energy, 2012. **86**(2): p. 771-779.
36. He, Q., et al., *Experimental investigation on photothermal properties of nanofluids for direct absorption solar thermal energy systems.* Energy Conversion and Management, 2013. **73**: p. 150-157.

37. Gupta, H.K., G.D. Agrawal, and J. Mathur, *An experimental investigation of a low temperature Al2O3-H2O nanofluid based direct absorption solar collector.* Solar Energy, 2015. **118**: p. 390-396.
38. Yousefi, T., et al., *An experimental investigation on the effect of Al2O3–H2O nanofluid on the efficiency of flat-plate solar collectors.* Renewable Energy, 2012. **39**(1): p. 293-298.
39. Said, Z., et al., *Performance enhancement of a Flat Plate Solar collector using Titanium dioxide nanofluid and Polyethylene Glycol dispersant.* Journal of Cleaner Production, 2015. **92**: p. 343-353.
40. Ghasemi, H., et al., *Solar steam generation by heat localization.* Nat Commun, 2014. **5**.
41. Jin, H., et al., *Steam generation in a nanoparticle-based solar receiver.* Nano Energy.
42. Neumann, O., et al., *Compact solar autoclave based on steam generation using broadband light-harvesting nanoparticles.* Proc Natl Acad Sci U S A, 2013. **110**(29): p. 11677-81.
43. Ni, G., et al., *Volumetric solar heating of nanofluids for direct vapor generation.* Nano Energy, 2015. **17**: p. 290-301.
44. Neumann, O., et al., *Solar vapor generation enabled by nanoparticles.* ACS Nano, 2013. **7**(1): p. 42-9.
45. Fang, Z., et al., *Evolution of Light-Induced Vapor Generation at a Liquid-Immersed Metallic Nanoparticle.* Nano Letters, 2013. **13**(4): p. 1736-1742.
46. Lukianova-Hleb, E., et al., *Plasmonic nanobubbles as transient vapor nanobubbles generated around plasmonic nanoparticles.* ACS Nano, 2010. **4**(4): p. 2109-2123.
47. Jin, H., et al., *Steam generation in a nanoparticle-based solar receiver.* Nano Energy, 2016. **28**: p. 397-406.
48. Jin, H., et al., *Photothermal conversion efficiency of nanofluids: An experimental and numerical study.* Solar Energy, 2016. **139**: p. 278-289.
49. Baffou, G., et al., *Super-heating and micro-bubble generation around plasmonic nanoparticles under cw illumination.* Journal of Physical Chemistry C, 2014. **118**(9): p. 4890-4898.
50. Carlson, M.T., A.J. Green, and H.H. Richardson, *Superheating water by CW excitation of gold nanodots.* Nano Letters, 2012. **12**(3): p. 1534-1537.
51. Lombard, J., T. Biben, and S. Merabia, *Kinetics of Nanobubble Generation Around Overheated Nanoparticles.* Physical Review Letters, 2014. **112**(10): p. 105701.
52. Hogan, N.J., et al., *Nanoparticles heat through light localization.* Nano Letters, 2014. **14**(8): p. 4640-4645.
53. Zhang, H., et al., *Dependence of Photothermal Conversion Characteristics on Different Nanoparticle Dispersions.* Journal of Nanoscience and Nanotechnology, 2015. **15**(4): p. 3055-3060.
54. Chen, H.-J. and D. Wen, *Ultrasonic-aided fabrication of gold nanofluids.* Nanoscale Research Letters, 2011. **6**(1): p. 198.
55. Xu, J., et al., *Design, Construction, and Characterization of an Adjustable 70 kW High-Flux Solar Simulator.* Journal of Solar Energy Engineering, 2016. **138**(4): p. 041010-041010.

List of Figures

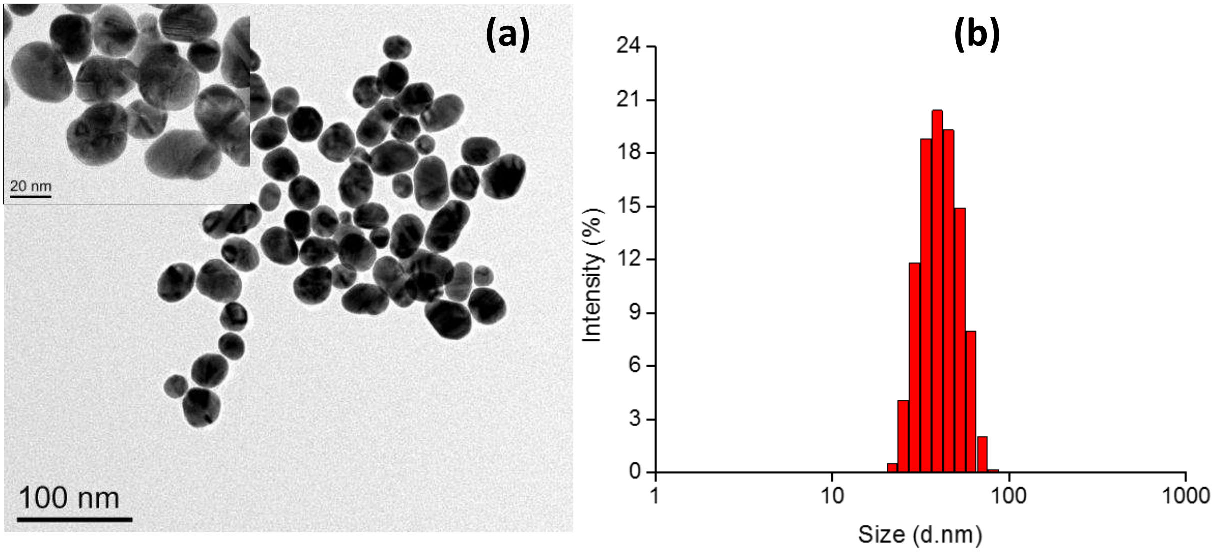

Fig. 1 Characterization of the synthesized gold nanoparticles, (a) TEM image of the gold nanoparticles showing a good suspension and size variation and (b) hydrodynamic size distribution of the gold nanoparticles measured by DLS.

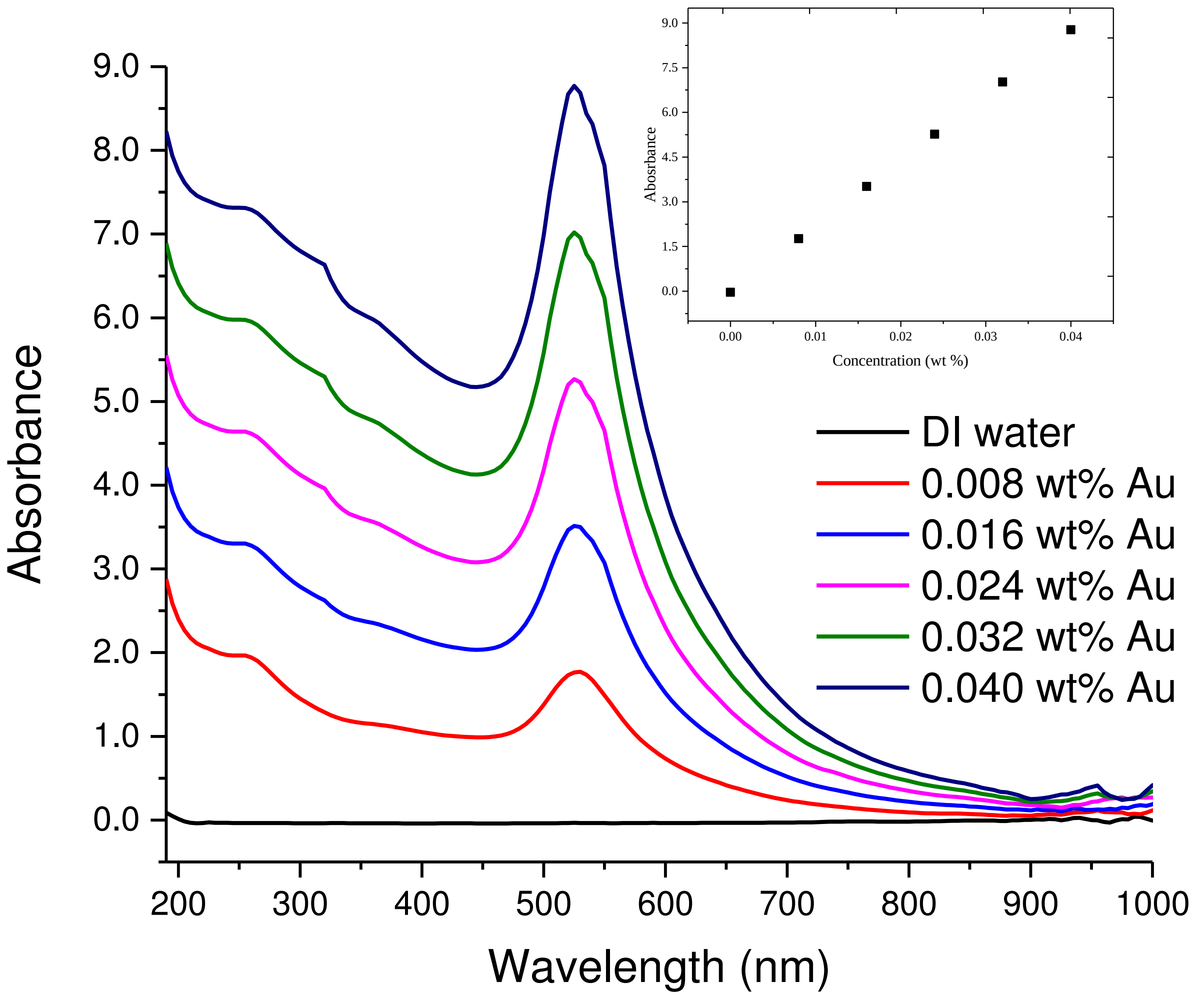

Fig. 2 Optical absorbance spectra of the gold nanofluids at various weight concentrations showing the absorbance peak at plasmonic resonance wavelength of 525nm. The inset shows a linear relationship of the absorbance peak with the concentration.

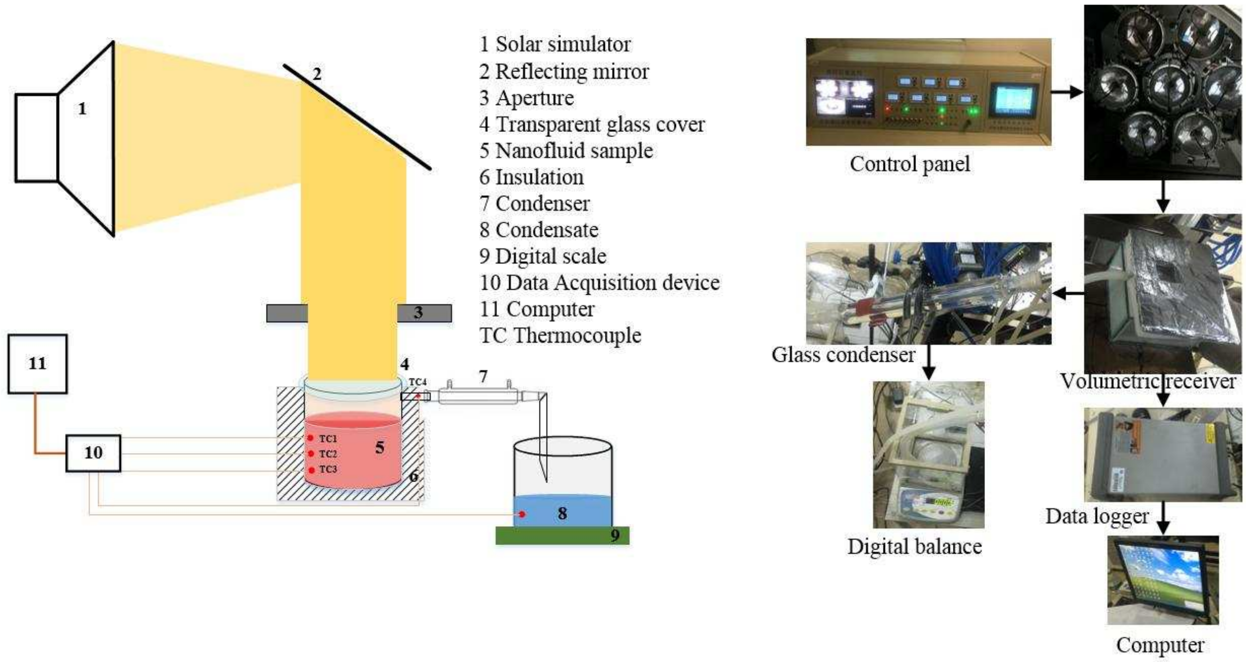

Fig. 3 Schematic of the experimental setup highlighting the major components.

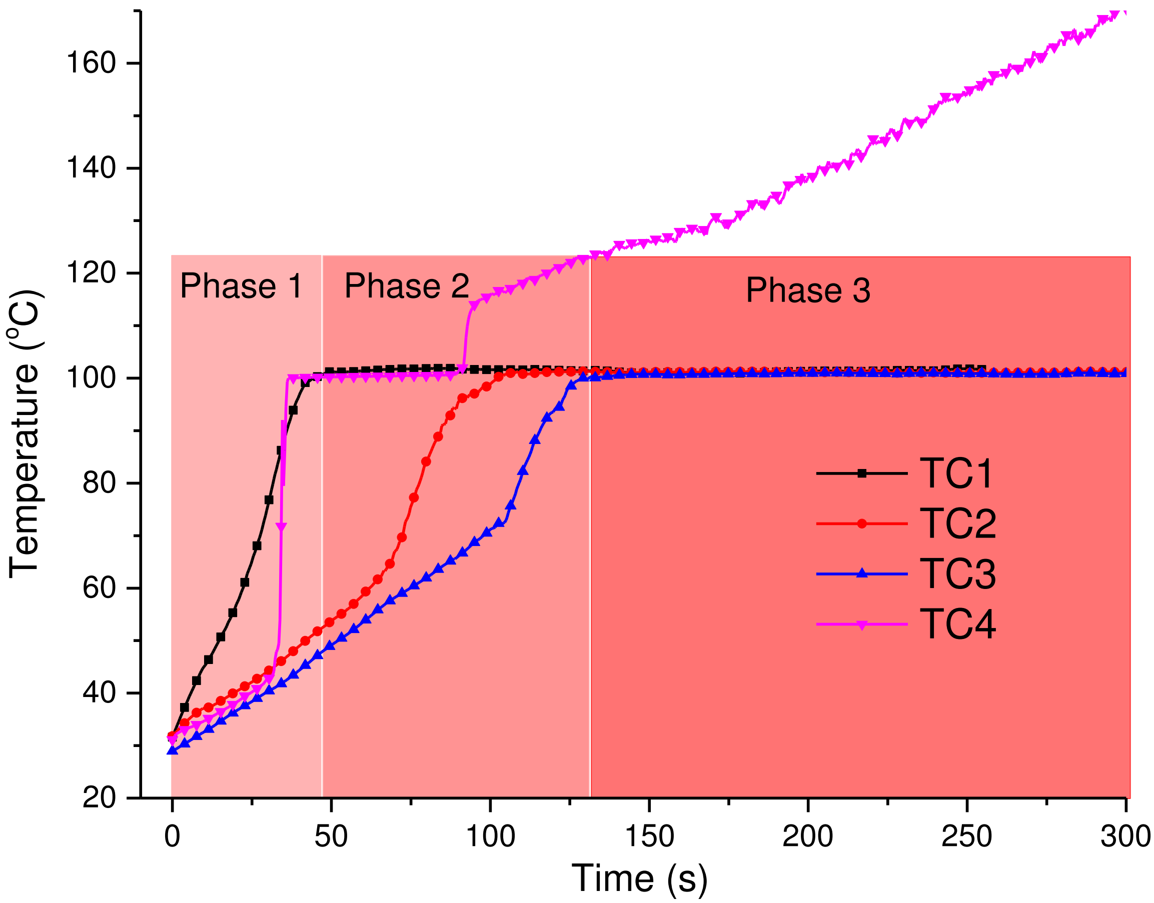

Fig. 4 Temperature distribution during the 5 min illumination of 0.016 wt% Au nanofluid sample where phase 1 shows the surface heating, phase 2 is the bulk fluid heating and phase 3 shows the saturated boiling of the sample. Here TC1, TC2 and TC3 are the temperatures of the thermocouples 1, 2 and 3 and TC4 is the temperature of the steam.

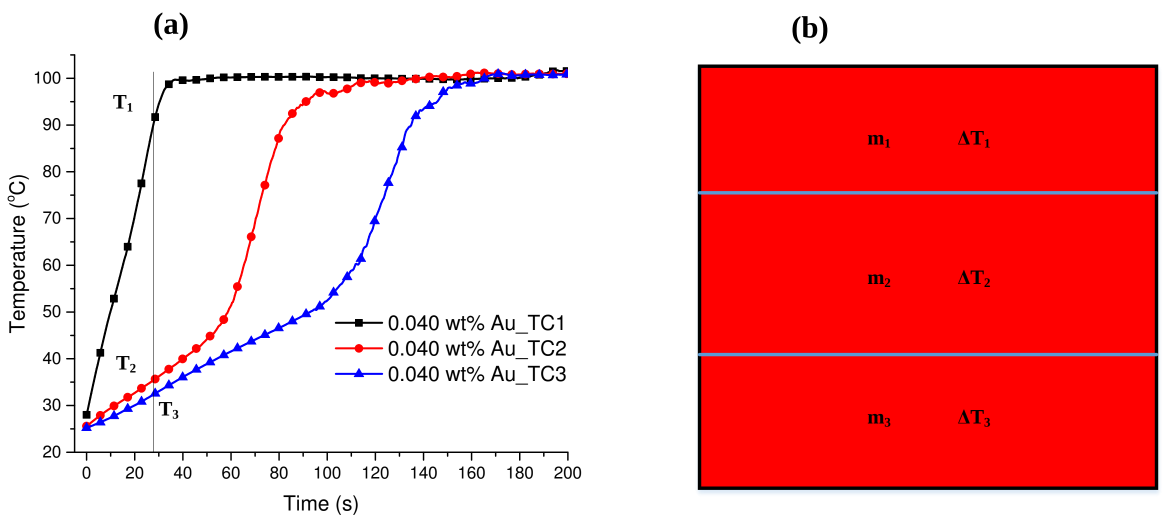

Fig. 5 (a) Variation of temperature along the depth of the 0.040 wt% Au nanofluid sample where T_1, T_2 and T_3 show the reading of thermocouples TC1, TC2 and TC3 respectively and (b) division of fluid volume into different levels as per the temperature distribution during fluid heating.

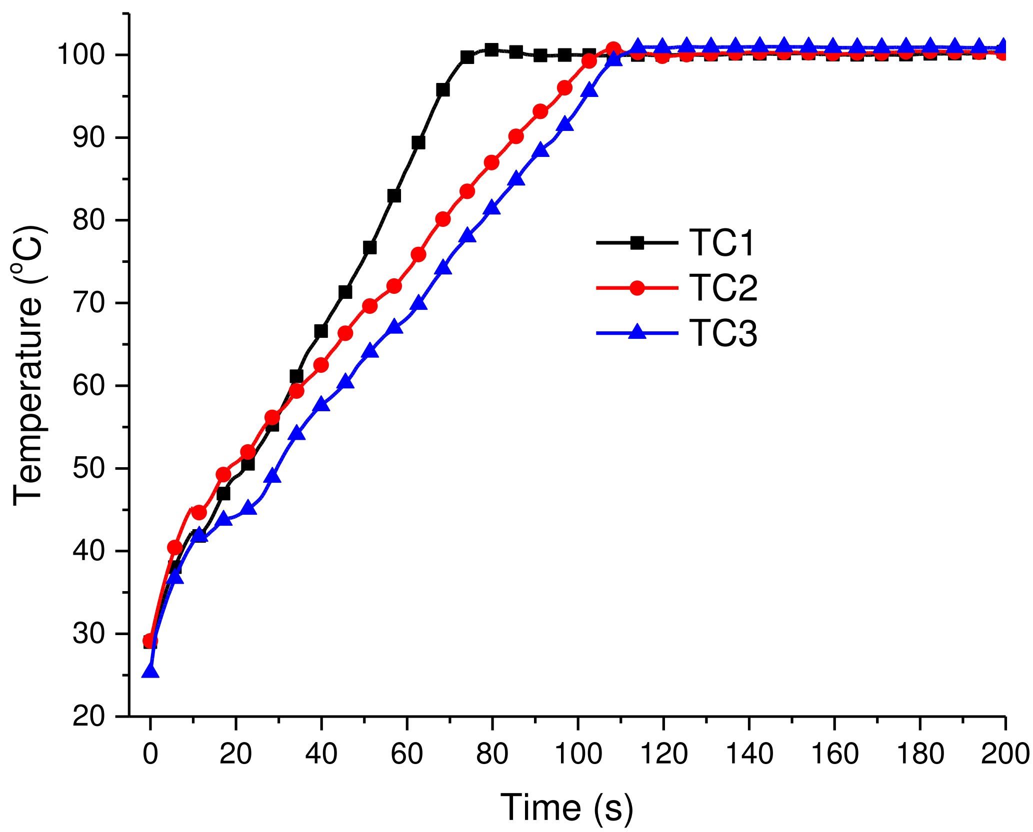

Fig. 6 Temperature distribution of the deionized water sample during the volumetric heating under the illumination of 280 Suns.

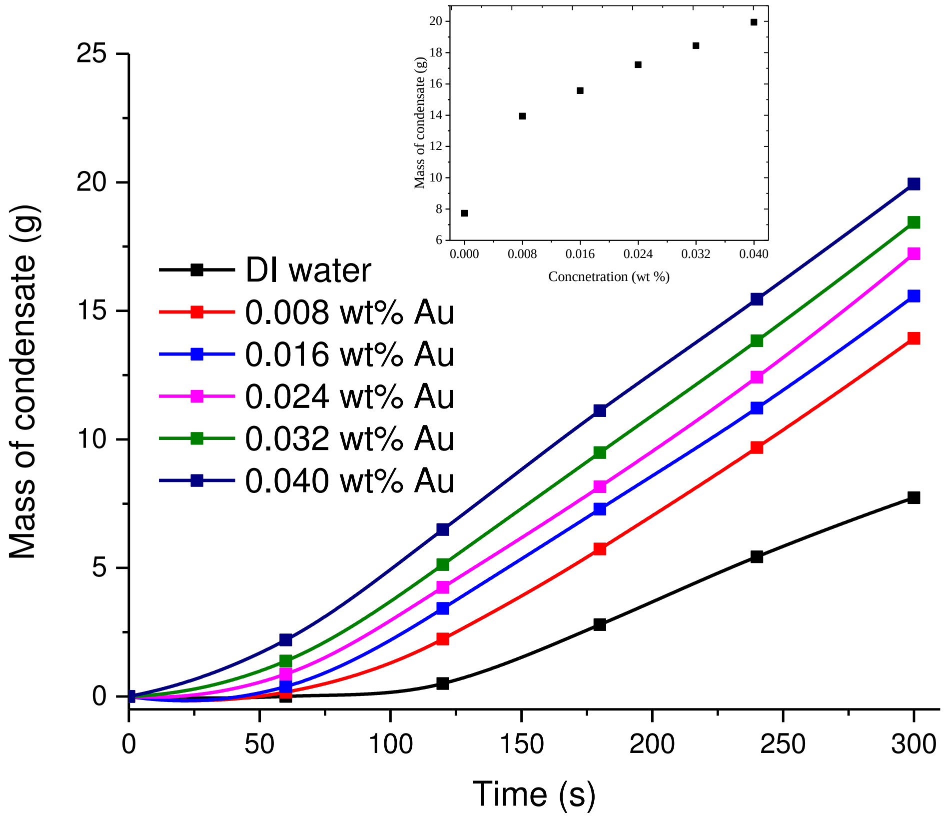

Fig. 7 Mass variation of the condensed vapors at different nanoparticle concentrations as the sample is illuminated with a radiation flux of 280 Suns for a period of 5 min.

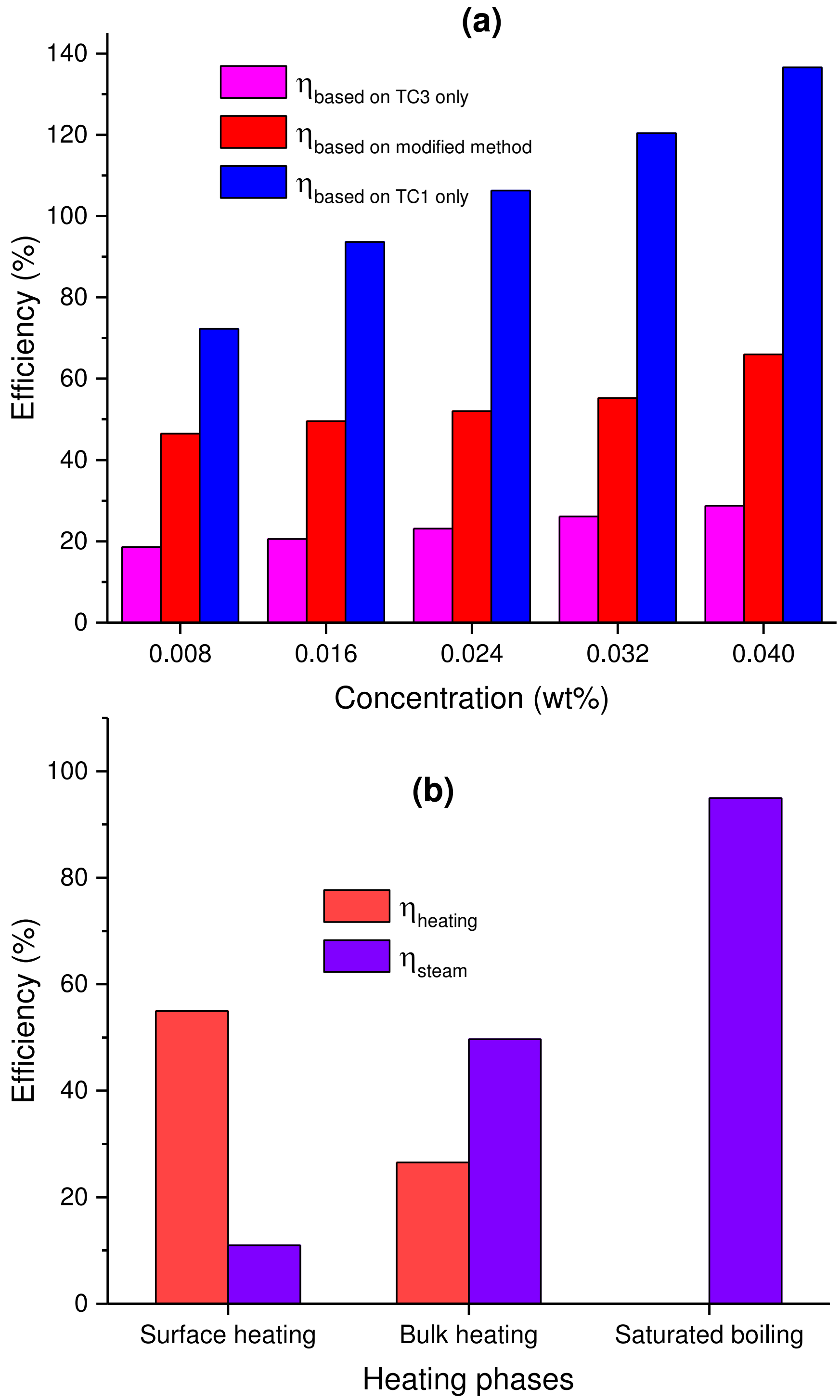

Fig. 8 (a) Efficiency (including latent heat) based on individual thermocouple and modified method at various nanoparticle concentrations during the phase 1 only and (b) Efficiency of sensible heating and steam generation during the three heating phases of 0.040% gold nanofluid sample where η_{heating} is based on modified method

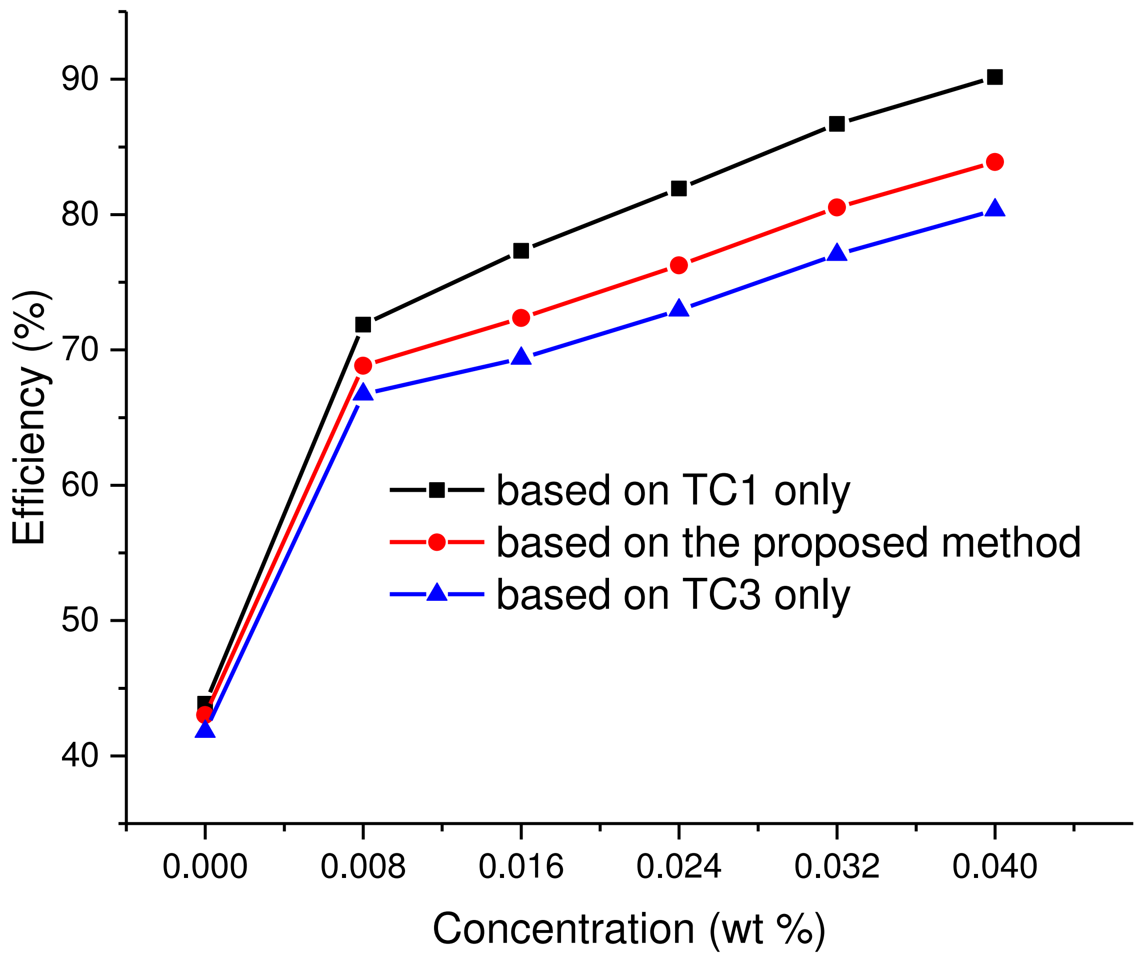

Fig. 9 Photothermal conversion efficiency (η_{PTC}) based on three methods at various nanoparticle concentrations over an irradiation time of 5 min.

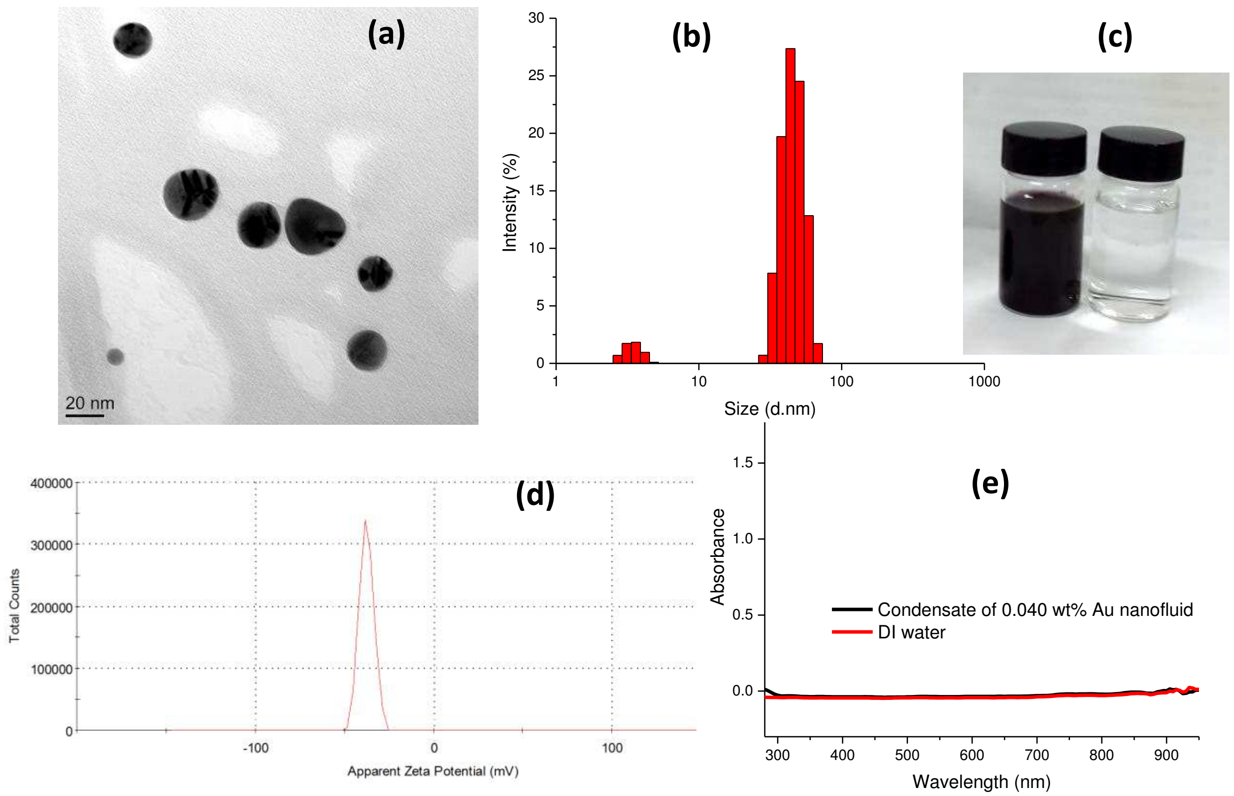

Fig. 10 Characterization of nanoparticles after the steam generation experiment. (a) TEM micrograph, (b) particle size distribution, (c) well stable concentrated left over gold nanosuspension (right) after evaporation and clear condensate (left), (d) zeta potential graph and (e) optical absorbance spectrum of the condensate showing the absence of nanoparticles as can also be seen from the clear color of condensate in (c).

Volumetric solar fluid heating and steam generation via based on direct solar absorptive gold nanofluids

Muhammad Amjad[1, 4], Ghulam Raza[1], Yan Xin[3], Shahid Pervaiz[1], Jinliang Xu[3], Xiaoze Du[3], Dongsheng Wen [2,1*]

[1] School of Chemical and Process Engineering, University of Leeds, Leeds, LS2 9JT, UK

[2] School of Aeronautic Science and Engineering, Beihang University, Beijing, 100191, P.R. China

[3] School of Energy, Power and Mechanical Engineering, North China Electric University, Beijing 102206, P.R. China

[4] Department of Mechanical, Mechatronics and Manufacturing Engineering (KSK Campus), University of Engineering and Technology Lahore, Pakistan.

.

Abstract: Volumetric solar absorption by using nanofluids can minimize the thermal losseses by trapping the light heat inside the fluid volumeand reducing the temperature difference between the absorbing surface and the fluid. A strong surface boiling of the nanofluid with the temperature of the underneath fluid still subcooled volume almost unchanged could an have many interesting applications, whose mechanism is still however under strong debate. This work advanced our understanding on volumetric fluids heating by performing a novel well-controlled experiment under a unique uniform solar heating setup at 280 Suns, with a particular focus on the steam production phenomenon using gold nanofluids. To take the temperature distribution into account, a new ovel integration method was used to calculate the sensible heating contribution. The results showed that the photothermal conversion efficiency was enhanced significantly by gold nanofluids. A three-stage heating scenario was identified and during the It was found that during the first stage， surface heating stage, most of the energy was absorbed by the surface fluid, resulting in rapid vapor generation, with the underneath fluid temperature in still subcooled state. The photothermal conversion efficiency was enhanced significantly by nanoparitclesnanoparticles, i.e. 95% over the base fluid for golda nanoparticle concentration of 0.040 wt%. The condensed vapor analysis showed no nanoparticle escaping even under vigorous boiling conditions. Such results reveal show that nanoparticle enabled volumetric solar heating surface boiling could have many promising applications including such as clean drinking water production in arid areas where abundant solar energy is available.

Keywords: Nanofluid, steam production, photothermal conversion, evaporation, direct absorption, solar energy

*Corresponding author. Tel.: 0044-113-3432678; fax: 0044-20-78825003.
Email address: d.wen@buaa.ac.uk / d.wen@leeds.edu.cn

Field Code Changed

1. Introduction

Solar energy is the most dominant renewable source that is available and accessible to everyone, but facing many ~~numerous~~ challenges to achieve ~~for its~~ efficient utilization [1]. Wide-spread solar powered applications are not limited to but consist of electricity generation [2, 3], ~~including~~ micro thermal power [4], chemical production line for ~~including~~ methanol [5] and hydrogen [6], water desalination [7-10], greenhouse growth in agriculture [11], sterilization [12] and cooling and refrigeration [13, 14]. The solar energy utilization of these applications can be significantly enhanced by suspending various nano-sized particles in a fluid, which is ~~and such solar receivers~~ called ~~are known as~~ direct absorption volumetric solar collectors [15-19]. In contrast to conventional solar collectors [20, 21] where the solar absorption is surface-based, i.e., having ~~with~~ large radiative and thermal losses due to ~~a~~ high~~er~~ surface temperature ~~especially for concentrated solar systems~~ [22], the volumetric solar collectors ~~not only~~ minimize these losses by thermal trapping [23, 24] and reduced ~~but also reduce the~~ temperature difference between the absorber and the fluid ~~interface temperature difference~~ [25, 26].

A variety of direct absorption nanoparticles ~~materials had~~ have been analyzed in terms of the enhancement in the photothermal performance, including Ag [27-29], Au [30-32], CNT (carbon nanotubes) [33-35], Cu [36], Al_2O_3 [37, 38], graphite [17], graphene [22], and TiO_2 [39]. In addition to the volumetric heating, direct vapor generation due to localized heating of ~~the~~

nanoparticles [40-43] is a recent development in this area. For example, Neumann et al.researchers [44] from Rice University showed that by using very dilute gold nanoparticles (16.7 ppm) under a focused solar light via a typical Fresnel lens, steam was produced instantly while the measured bulk temperature was still 6 ^{o}C approximately. The calculated steam generation efficiency reached 80%, meaning only 20% of the solar radiation was used to increase the bulk fluid temperature. Later simulation work [44-46] showed the possibility of nanobubble formation based on a non-equilibrium phase change assumption. However these results are quite different to the recent results from Jin et al. [47]. Still using a Fresnel lens (i.e. solar flux ~220 Suns), it revealed that steam generation was mainly caused by localized boiling and evaporation in superheated regimes due to a highly non-uniform temperature distribution, albeit the bulk fluid was still subcooled. The, and the hypothesized nanobubble, i.e., steam produced around heated particles, was unlikely to occur under normal solar radiations. It shall be noted that all these experiments [44, 47, 48] were performed outdoor, where the solar flux may variedy from time to time, and the focus by Fresnel lens limited the heating to a small area, leading to a non-uniform solar energy input. Such would lead to a very high solar flux in localized areas (i.e. spot heating), producing spot heating and leading to high evaporation rate locally. It is however unclear if a similar phenomenon could be observed under a uniform solar heating.

As far as the steam generation mechanism is concerned, for nanobubbles to be produced around heated nanoparticles, it has been shown analytically that a minimum radiation flux of 3×10^{8} W/m^2 is required to produce nanobubbles on heated nanoparticles [46, 49, 50], which can may only be reached developed by powerful laser beams. In a separated theoretical study, of the nanobubble development kinetics around plasmonic gold nanoparticle by Julien et al. [51] showed that to generate a nanobubble, a flux intensity of around 1×10^{10} W/m^2 was required to generate a nanobubble on a plasmonic gold nanoparticle. However quite differently, Hogan et al. [52] reported that ~ 1 MW/m^2 solar reflux was sufficient for efficient steam production due to a collective effect of nanoparticles that both scatter and absorb light, hence localizing light energy into mesoscale volumes.

It shall be noted that most of the experiments performed so far were not under well-controlled conditions [44, 47, 48]. Beside the problem of a varying solar flux and spot heating mentioned above, most of the experiments were performed bywith a single-point temperature measurement, ignoring the actual temperature distribution in the bulk fluid [32, 44, 53]. Though Jin et al. [41] and Ni et al. [43] used multipoint temperature measurement, only the average temperature was used for the evaluation of the photothermal efficiency. In Jin's work [41], the spot heating and small fluid volume minimized the temperature stratification phenomenon, and the fluid led to a rapid reached ing to the saturated boiling rapidlystatus , where the most interesting phenomenon under subcooled condition was insufficiently captured. In addition, possible escaping phenomenon of nanoparticles with the steam under saturated boiling has not been investigated, which is critical for any potential desalination or clean drinking water production applications. Clearly a better understanding of the solar steam generation by nanoparticles is much needed.

This work aims to advance the field by answering three questions: i) Would Could significant the steam generation phenomenon be different under be produced under a uniform solar heating, instead of spot heating? ii) What is the underneath mechanism for steam production if not by forming nanobubbles? and iii) Would nanoparticle be escaped with the produced steam? To answer chieve these questionsgoals, we performed a well-controlled steam generation experiment under a unique high power solar simulator (i.e. up to 4 MW/m^2) with , which has a large focus area to provide uniform heating. A novel one-dimension test section was designed, and multiple thermocouples were used to reveal the temperature distribution along the heating path. A novel integration method was proposed to calculate the sensible heating contribution and to aid the analysis of steam production mechanism. Various concentrations of gold nanofluids were produced and used as the test fluids, and the generated steam was condensed to reveal the presence of any nanoparticles. All sample nanofluids before and after the experiment ~~–~~were carefully ~~ompletely~~ characterized in terms of stability, size distribution and morphological variation. Such would allow us to answer the proposed questions and advance the solar applications by ~~of~~ direct absorption nanofluids.

2. Materials and methods

2.1. Reagents and devices

Hydrogen tetrachloroauric acid ($HAuCl_4$, Au ⩾ 49%) and Tri-sodium citrate ($Na_3C_6H_5O_7$, 99.8%) were purchased from ~~supplied by~~ Fisher Scientific and ~~were~~ used as received. Deionized water was used throughout the experiments~~al procedure~~.

A transmission electron microscopy (TEM) (TECNAI, TF20) equipped with EDX (Energy Dispersive X-ray spectroscope), was used to analyze the morphology ~~ical appearance~~ of the synthesized nanoparticles. The concentration of the gold dispersion was determined ~~checked~~ by an ~~with~~ Atomic Absorption Spectrometer (AAS) (VARIAN, AA240FS). The hydrodynamic size and zeta potential of the nanofluids were obtained ~~were analyzed using~~ by a DLS (dynamic light scattering) device (Malvern nanosizer). The optical absorption of the nanofluid was examined ~~checked on~~ by a UV/Vis spectrophotometer (HITACHI, U-3900) using a high precision cell with light path of 10mm.

2.2. Nanofluid synthesis and characterization

Gold nanoparticles (GNPs) were synthesized by the one-step method based on ~~using~~ a ~~slightly~~ modified thermal citrate reduction method ~~of $HAuCl_4$~~ as reported by Zhang at el. [32] and Chen et al. [54]. In the synthesis process, 100 ml of 5mM $HuACl_4$ solution was mixed with 100 ml of 10 mM trisodium citrate solution. The resultant mixture was heated to the boiling point until the mixture turned to wine red color. The resultant solution was continuously heated at 80 °C in a sonication bath for further 3 hours. Synthesized GNPs were aged at room temperature for 24 hours and ~~then~~ cleaned by ~~through membrane~~ the dialysis from ~~using~~ 8 kD~~d~~a membrane ~~and deionized (DI) water~~. The membrane allows the excessive ions to diffuse smoothly from the suspension and blocks the GNPs. DI water was changed twice a day for a period of 10 days, leading to pure ~~. Thus the suspension contains only~~ GNPs dispersions. The concentration of the resulting nanofluid ~~suspension~~ was measured by Atomic Absorption Spectrometry (AAS).

The morphology~~ical characterization~~ of the synthesized nanoparticles was analyzed by a ~~transmission electron microscopy (~~TEM~~)~~ and the hydrodynamic size was measured by the DLS ~~(dynamic light scattering)~~ device. **Fig 1 (a)** shows the TEM image of the nanoparticles and the inset shows a ~~more~~ close view. It can be seen that the gold nanoparticles are mostly ~~of~~ spherical ~~shape~~ with particle size in the range of ~~and varies in size ranging from~~ 20~ ~~to~~ 30 nm. The hydrodynamic size distribution of the gold particles, ~~is shown in~~ **Fig. 1 (b)**, shows a slightly ~~. The size of the particles suspended in deionized water measured by DLS is slightly~~ larger size than that from ~~e~~TEM ~~size~~, which is due to ~~which is because of~~ the hydrodynamic nature of size measurement by ~~of~~ DLS.

The optical absorbance of Au nanofluids was checked by ~~on~~ UV/Vis spectrophotometer (U-3900, HITACHI) using a high precision cell with light path of 10 mm. The a~~A~~bsorbance is defined as the logarithm (10 as base) of reciprocal of transmittance, whereas the transmittance is the ration of the transmitted light by the nanofluid sample to the incident light on it. According to the Beer-Lambert's Law [53], absorbance is $log\,(I_o/I) = \epsilon lc$, where I_o is the incident light on the sample, I is the light transmitted by the nanofluid sample, ϵ is the extinction coefficient, l is the length of the sample through which light passed, and c is the concentration of the nanofluid. The absorbance of Au nanofluids is shown in **Fig.2**, where the inset shows a linear relationship of the absorbance peak with the concentration. The absorbance peak of the Au nanofluid appears at a wavelength of 525 nm and is identical for various concentrations. The absorbance peak can be engineered widened and shifted towards longer wavelength having relatively larger amount of energy in the visible spectrum by controlling the size and shape of the nanoparticles during the synthesis process.

2.3. Experimental setup

Photothermal conversion characteristics and steam generation capability of the characterized gold nanofluids were investigated using a solar simulator having seven xenon short-arc lamps aligned on the reflector ellipsoidal axis [55]. The solar simulator is capable of producing a concentrated solar flux of about 4 MW/m^2 when all of seven lamps are in operation, for more details about the solar simulator, please refer to **Section I of the supplementary information**. Only one lamp was put in operation for the current experiments to deliver a solar flux equivalent to 280 Suns in the current study. The solar radiation had a focal area of 28.27 cm^2, which was passed through a custom-made aperture (30 mm diameter) of aerogel sheet wrapped in aluminum foil. The test section was made of high temperature quartz glass with the inner and outer diameter of 30 mm and 34 mm respectively. The test section was put accurately under the solar radiator to enable a uniform heating. A sample fluid of 25 ml (~35.4 mm depth) was filled into and covered with a transparent quartz cover. Holes of 1 mm diameter were fabricated in the vessel to insert the thermocouples equidistant to each other at 10 mm. The vessel was covered with a tightly packed aerogel blanket with thermal conductivity of ~~as low as~~ 0.015W/m^{2}K to minimize the heat loss to the surroundings. A square glass box was used to contain the aerogel with the vessel fitted in a hole in the aerogel sheets, and further details can be seen in **Section II of the supplementary information**.

Three K-type (Omega 5TC-TT-K-36-36) thermocouples (TC) were used to measure the bulk fluid temperature, positioned evenly along the optical depth in top, middle and bottom sections of the sample fluid at distance of 10 mm from each other. This was to ensure ~~such~~ that neither the top TC ~~thermocouple~~ was exposed to the air during ~~at the beginning of~~ the experiment nor the bottom ~~lower most~~ TC ~~was~~ touched ~~ing~~ the bottom of the vessel. The temperature of the vapor generated was measured through an additional K-type thermocouple. The steam temperature was measured ~~as at~~ at the middle of a 20 mm long exit channel, ~~of the vessel~~ as shown in ~~the schematic in~~ **Fig. 3**. The temperature ~~data~~ was ~~ere~~ registered by a data logger (Agilent 34970A) linked to a ~~the~~ computer ~~for its measurement and monitoring~~. The uncertainty in temperature measurement was validated as ±0.25 K ~~°C~~. The generated steam was condensed in a glass condenser with cooling water circulating around the condensing tube. A sensitive digital ~~weight~~ balance (Setra, BL-500S) with uncertainty of ±0.001g was used to measure the mass ~~weight~~ of the condensed vapors. ~~The experimental setup is highlighted schematically in **Fig.3**.~~

3. Results and discussion

3.1. Fluid heating and steam characterization

The bulk fluid temperature was measured by three thermocouples TC1, TC2 and TC3 as the nanofluid sample was heated under a solar flux of 280 Suns. from the solar simulator. The top TC1 being close to the top surface showed a rapid change in fluid temperature as the sample is illuminated. Depending upon the variation of bulk fluid temperature, **Fig.4**, as it is irradiated, the fluid heating can be divided into three phases. The first phase is the heating of surface fluid with the underneath fluid in subcooled condition. The surface fluid reaches to the boiling temperature rapidly in a very short span of time and the temperature of the underneath layers of the fluid volume is- slightly changed **(Fig. 4 and Fig. 5).** The second phase is the heating of bulk fluid volume in which the heat flux penetrates and brings the temperature of the whole fluid volume to the boiling point. The third phase is the saturated boiling phase in which the sample volume temperature reaches the boiling point. boils from the surface to the bottom. Due to the superheating, tThe steam temperature continues to increase above the boiling temperature of the fluid untill the radiation flux is switched off. as can be seen in **Fig.4**. This shows that steam undergoes some degree of superheating during the experiment. The temperature distribution in the first two heating phases can be clearly seen in **Fig. 5 (a)**, in which the concentration of gold nanoparticles is 0.04 wt%. The non-uniformity of temperature along the heating path fluid depth is increased directly with the increase of gold nanoparticle concentration. This is fact can be associated with the increased radiation absorption at the surface of maximum of radiation flux by the surface nanofluid due to more solar energy trapping at the surface at a higher concentration. due to increased density of gold nanoparticles in surface layer as the weight concentration is increased. The temperature distribution for deionized water sample is shown expressed in **Fig. 6** as a comparison, and more non-uniform temperature profile can be referred to for reference and **Section III of the supplementary information**. can be referred for more non-uniform temperature profiles. It is evident from Fig. 6 that the radiation flux is passed through the for DI water, sample layers and there is no there is not much significant temperature variation along the heating path sample depth during the initial volumetric heating phase. The Also the rate of rise in surface temperature in case of DI water is also much slower very far low than that of 0.040 wt% gold nanofluid **(Fig. 5a)**

The energy absorbed by the nanofluid sample in the sensible heating was calculated using the following relation in their studies done by Zhang et al. [32, 53] and Neumann [44], where only one temperature sensor was used to represent the bulk fluid temperature;

$$Q = c_p m \Delta T \quad (1)$$

where c_p, m and ΔT are the specific heat capacity, mass of the sample taken and temperature change of the fluid volume over the specified time. The change in temperature ΔT was replaced by $\Delta \bar{T}$, the average change in temperature in the study done by Jin et al. [41, 48] in which more than one thermocouple were used for the measurement of fluid temperature. As clearly seen from **Fig. 5 (a)** that the fluid temperature is not highly non-uniform, the temperature measured by only one thermocouple is clearly not capable of representing the fluid temperature. The calculated absorbed energy may be overestimated or under estimated depending upon the position of the thermocouple. Even the average value of the temperature may also be misleading depending upon several factors, including type of nanoparticles, their concentrations, color of the nanofluid and intensity of radiation flux.

Here we used a more realistic method to calculate the energy absorbed by the nanofluid volume especially at high nanoparticle concentrations. The fluid volume is divided into various temperature dependent sections as shown in **Fig. 5(b)**. The absorbed energy of the each section can be calculated independently and the overall absorbed energy can be evaluated using the relation given in Eq. 2;

$$Q = c_p \sum_{i=1}^{n} (m_i \Delta T_i) \qquad (2)$$

and the overall photothermal conversion efficiency (η_{PTC}) including sensible heating and latent heat can subsequently be calculated from Eq. 3;

$$\eta_{PTC} = \frac{c_p \sum_{i=1}^{n}(m_i \Delta T_i) + \int_0^t L_v m_v dt}{\int_0^t I A_a dt} \qquad (3)$$

where I is the solar irradiance, A_a is the area of the aperture, L_v is the latent heat of vaporization of water and m_v is mass of the condensed vapors in time dt. Although the thermophysical properties of water like thermal conductivity and specific heat capacity would be are changed with the addition of nanoparticles. However but with such a very small nanoparticle concentration (0.040 wt%), the change in these properties was found to be negliblenegligible. The mass of the condensed vapor generated as the nanofluid samples with different nanoparticle weight concentrations radiated at a flux of 280 Suns over a 5--min duration is given in **Fig. 7**, which shows a siginificanlty higher value for . The mass of vapor condensate of nanolfuidnanofluid samples is siginificanlty higher than that of deionized water. Comparing with DI water, aAn enhancement of 80% and 157% in the vapor generation efficiency are observed for gold nanofluids at for nanolfuidnanofluid sample with concentration of 0.008 wt% and about 157% with concenetration concentration of 0.040 wt% respectivelywas observed over deionized water. The The amount of condensed vapor is increased s is nearly linearly with the increase of directly related to the concentration of the gold nanoparticle concentration,s as presented in

Fig.7 (inset). The variation in the mass of condensate at the inititial volumetric heating of the samples with varying concentration is small, which might be due to the recondensation of the vapors. The vapors generated under subcooled conditions have greater ~~tendancy~~tendency of recondensation due to the presene of cold vessel walls. A constant evaporation rate after the phase two ~~2~~ of the volumetric heating confirms the saturated boiling in the nanofluid sample. The uncertainty in the mass measurement for the sample with 0.008 wt% nanoparticle concentration was estimated to be ±0.592% for the first 60 seconds of illumination. The relative uncertianty in the calculated photothermal efficiency was estimated to be ±2%, and detailed uncertainty analyiss can be found in the ~~refer to~~ **Section IV of the supplementary information** ~~for uncertainity analysis in measurements and calculations.~~

~~-~~The energy absorbed by the nanofluid ~~sample~~ during ~~in the~~ the sensible heating period was calculated using the following relation ~~in their studies done~~ by Zhang et al. [32, 53] and Neumann [44], where only one temperature sensor was used to represent the bulk fluid temperature;

$$Q = c_p m \Delta T \qquad (1)$$

where c_p, m and ΔT are the specific heat capacity, mass of the sample taken and temperature change of the fluid volume over the specified time. The change in temperature ΔT was replaced by $\Delta \overline{T}$, i.e., the average temperature difference ~~change in temperature in the study done~~ by Jin et al. [41, 48], in which more than one thermocouple were used ~~for the measurement of fluid temperature~~. As clearly seen from **Fig. 5 (a)** that the fluid temperature is highly non-uniform, the temperature measured by only one thermocouple is clearly not ~~capable of~~ representing the fluid temperature. The calculated absorbed energy may be overestimated or under~~-~~estimated depending upon the position of the thermocouple. Even the average value of the temperature may also be misleading depending upon several factors, including the type of nanoparticles, their concentrations, color of the nanofluid and intensity of radiation flux.

Here we used a more realistic method to calculate the energy absorbed by the nanofluid volume especially at high nanoparticle concentrations. The fluid volume is divided into various temperature dependent sections as shown in **Fig. 5(b)**. The absorbed energy of the each section is can be calculated independently and the overall absorbed energy can beis evaluated using the relation given in Eq. 2;

$$Q = c_p \sum_{i=1}^{n} (m_i \Delta T_i) \quad (2)$$

and . The the overall photothermal conversion efficiency (η_{PTC}) including sensible heating and latent heat is can subsequently be calculated from Eq. 3, which is a modified version of the equation used by Jin et al. [41];

$$\eta_{PTC} = \frac{c_p \sum_{i=1}^{n}(m_i \Delta T_i) + \int_0^t L_v m_v dt}{\int_0^t I A_a dt} \quad (3)$$

where I is the solar irradiance, A_a is the area of the aperture, L_v is the latent heat of vaporization of water and m_v is mass of the condensed vapors in time dt.

Fig 8 (a) shows the photothermal conversion efficiency during the first phase, i.e. surface heating which is typically less than achieved in not more than 30 seconds after the of the illumination time. heating. -The efficiency includes the sensible and latent heat contributionss during this very short span of time. As can be observed in **Fig 8 (a)** that the position of the thermocouple has a great influence in determining the photothermal efficiency. If only one thermocouple is used for the measurement of temperature change as in [32, 44, 53] and the optical length of the fluid volume is significant, the obtained photothermal efficiency would be ~~may be misleading due to~~ underestimated ~~ion~~ if the thermocouple is away from the surface (as TC3 here in this study) and overestimated ~~ion~~ (as TC1 in this study) if it is close to the surface. ~~This is because the temperature distribution does has a significant influence on the photothermal efficiency. So in this case, using multiple thermocouples that divide the fluid volume into multiple sections is advisable.~~

~~As in **Fig. 8 (a)**, the efficiency based on TC3 only is an underestimation because of the uneven temperature distribution and the efficiency based on TC1 only is clearly an overestimation because the heat is abosrbed by the surface layer of the fluid only and its dissipation to the lower layers is restricted.~~ This underestimation or overestimation is because the ~~temperaure~~ temperature of the respective thermocouple is used to represent ~~thought to be~~ the temperature of the whole fluid volume at any instant, but actually it is not as already shown~~in~~ in **Fig. 5 (a)**. Using the proposed ~~modified~~ method of calculating the photothermal efficiency, i.e. taking the temperature distribution into account, gives more realiable results and is necessacitated particulary when the temperature remains below ~~under~~ the boiling temperaure of the nanofluid.

Fig 8 (b) shows in the efficiency of sensible heating and steam generation in the proposed three phases (**Fig. 4**) during the irradiance time of 5 min for a nanoparticle concentration of 0.040 wt%. D~~d~~uring the surface heating, most of the absorbed energy is used in the sensible heating of the ~~nanolfuid~~nanofluid, together with some vapor~~s~~ generated.~~ in the top of the nanoparticles~~ while in case of DI water, ~~basefluid~~ no vapor~~s~~ were observed in the surface heating phase. Hence the presence of nanoparticles ~~ehnaces~~enhances the steam genergation efficiency even under subcooled condition as also observed ~~mentioned~~ by Jin et al. [41]. The steam generation efficiency of about 95% in the saturated boiling is very attractive and gives an enhancement ~~of~~ of 117.5% over the base fluid.

Fig. 9 shows the overall efficiency of the plasmonic gold nanofluid at various concentrations compared to the base fluid. The photothermal efficiency is dramatically enhanced by ~~on adding~~ gold nanoparticles ~~in the base fluid~~. At a particle concentration of 0.040 wt%, the overall photothermal efficiency or in a broader term the energy efficiency is enhanced by 95% over the base fluid in the experimental domain. This enhancement increases almost linearal~~l~~y with the nanoparticle concentration. It can also be noticed that the efficiency difference among the three modes of its evaluation is negligibly small when there is no nanoparticle in the base fluid. But with the addition and increase in the concentation of the nanoparticles~~ in the base fluid~~, this difference is magnified. This is due to the non-uniform ~~uneven~~ temperature distribution (**Fig. 4**) ~~which is because of~~ caused by the presence of the ~~plasmonic~~ nanoparticles~~ in the basefluid~~. This non-uniform temperature distrbution is very supportive in evaporating the fluid from the surface while ~~and~~ keeping the bulk volume under subcooled conditions. This phenomenon can be used to produce clean ~~drinking~~ water by ~~evaorating~~ evaporating the water from the surface and keep circulating the underneath volume like in forward osmosis desalination.

3.2. Analysis of nanoparticles after experiments

The remaining ~~left over~~ concentrated nanosuspension after the experiments was examined in terms of stability, nanoparticle size distribution and morphological appearance it had undergone. ~~**Fig. 10** shows the characterization of the residual nanofluid.~~ **Fig 10 (a)** and **(b)** represents the TEM micrograph and hydrodynamic size distribution of the particles after ~~cooking~~ boiling repectively. Compared with the characterization results before the experiment, the size and shape of the gold nanoparticles is almost the same ~~–~~after the ~~steam generation~~ experiment. The hydrodynamic size distribution of the nanoparticle is slightly changed and has a maximum intensity at 44 nm, which was at 49 nm before the experiments. The size inensity distribution is more compact and peaked after the photothermal coversion experiments. An additional smaller peak is observed in the DLS size distribution. This might be due to the ~~clapse~~ collapse of the surfactant layer on the surface of the nan~~a~~oparticles. The zeta potential of the nanofluid after the steam generation experiement is about -37 mV as shown in in Fig. **10 (d)**, which indicates a good stability of the suspension.

As to the possible nanoparticle entrainment ~~phenomeon~~phenomenon, **Fig. 10 (c)** shows that the ~~left over~~~~leftover~~ remaining concentrated gold nanofluid in dark red wine color and the condensate in transparent. The UV/Vis spectrum of the condensate presented in **Fig 10 (e)** also confirms that no particles were blown out with the steam even~~ ven~~ under strong boiling conditions. This phenomon is ~~be~~ very helpful for solar desalination applications, where potable water could be produced following vapor generation, induced by highly absorptive nanopaticles ~~in the water mixture.~~.

4. Conclusion

A well-controlled steam generation experiment was performed ~~and the effect of non-uniform temperature distribution during the bulk fluid heating on the photothermal conversion efficiency and enhanced vapor generation performance of~~ by using gold nanofluids ~~was investigated~~ under a concentrated solar flux of 280 Suns, and the main conclusions can be summarized: ~~.~~

- Highly non-uniform ~~A very clear uneven~~ temperature distribution was found ~~present~~ along the heating path of gold nanofluids~~in the layers of the nanofluid sample before the~~

Formatted: Font: Not Bold

Formatted: List Paragraph, Bulleted + Level: 1 + Aligned at: 0.63 cm + Indent at: 1.27 cm

Formatted: Font: (Default) Times New Roman, 12 pt

Formatted: Font: (Default) Times New Roman, 12 pt

~~saturated boiling stage was obtained.~~ and an integration method was proposed to calculate the sensible heating contribution.

- ~~During~~ Three phases of heating was identified, i.e., surface heating, subcooled boiling and saturated boiling. During the surface heating phase~~stage~~, most of the energy was absorbed by the surface fluid, resulting in vapor generation while ~~, still keeping~~ the underneath fluid still subcooled. ~~Due to non-uniform temperature distribution, an integration method to calculate the sensible heating contribution should be used instead of relying on one point temperature measurement~~.
- The p~~P~~hotothermal conversion efficiency and steam generation performance ~~of the base fluid is significantly enhanced with the addition of gold nanoparticles and~~ increased s almost linearly ~~directly~~ with the increase of particle concentration. An enhancement in the energy efficiency of about 95% over the base fluid was achieved for ~~with a~~ 0.04 wt% ~~of~~ gold nanofluids~~particles was achieved~~.
- The analysis of the condensed vapor proved the absence of gold nanoparticle, suggesting that the nanoparticles were not entrained by the vapor even under vigorous boiling.

Formatted: Font: (Default) Times New Roman, 12 pt

Formatted: Font: (Default) Times New Roman, 12 pt

Formatted: Font: (Default) Times New Roman, 12 pt

Formatted: Font: (Default) Times New Roman, 12 pt

Formatted: Font: (Default) Times New Roman, 12 pt

Formatted: Font: (Default) Times New Roman, 12 pt

Formatted: Font: (Default) Times New Roman, 12 pt

Formatted: Font: (Default) Times New Roman, 12 pt

Formatted: Font: (Default) Times New Roman, 12 pt

Formatted: Font: (Default) Times New Roman, 12 pt

Formatted: Font: (Default) Times New Roman, 12 pt

Formatted: Font: (Default) Times New Roman, 12 pt

Acknowledgement

The authors acknowledge the support from University of Engineering and Technology Lahore in collaboration with Higher Education Commission of Pakistan under Faculty Development Program, the National Science Foundation of China (Grant No. 51228601) and British Council Newton Fund-PhD Placement Grant (Grant No. 473117) for this work.

References

1. Modi, A., et al., *A review of solar energy based heat and power generation systems.* Renewable and Sustainable Energy Reviews, 2017. **67**: p. 1047-1064.

2. Manente, G., *High performance integrated solar combined cycles with minimum modifications to the combined cycle power plant design.* Energy Conversion and Management, 2016. **111**: p. 186-197.
3. Gupta, M.K. and S.C. Kaushik, *Exergy analysis and investigation for various feed water heaters of direct steam generation solar–thermal power plant.* Renewable Energy, 2010. **35**(6): p. 1228-1235.
4. Maghanki, M.M., et al., *Micro combined heat and power (MCHP) technologies and applications.* Renewable and Sustainable Energy Reviews, 2013. **28**: p. 510-524.
5. Bai, Z., et al., *A polygeneration system for the methanol production and the power generation with the solar–biomass thermal gasification.* Energy Conversion and Management, 2015. **102**: p. 190-201.
6. Ozturk, M. and I. Dincer, *Thermodynamic analysis of a solar-based multi-generation system with hydrogen production.* Applied Thermal Engineering, 2013. **51**(1–2): p. 1235-1244.
7. Tiwari, G.N., H.N. Singh, and R. Tripathi, *Present status of solar distillation.* Solar Energy, 2003. **75**(5): p. 367-373.
8. Ali, M.T., H.E.S. Fath, and P.R. Armstrong, *A comprehensive techno-economical review of indirect solar desalination.* Renewable and Sustainable Energy Reviews, 2011. **15**(8): p. 4187-4199.
9. Gude, V.G., N. Nirmalakhandan, and S. Deng, *Desalination using solar energy: Towards sustainability.* Energy, 2011. **36**(1): p. 78-85.
10. Shannon, M.A., *Water desalination: Fresh for less.* Nat Nano, 2010. **5**(4): p. 248-250.
11. Hassanien, R.H.E., M. Li, and W. Dong Lin, *Advanced applications of solar energy in agricultural greenhouses.* Renewable and Sustainable Energy Reviews, 2016. **54**: p. 989-1001.
12. Dravid, M.N., et al., *The use of solar energy for powering a portable autoclave.* Journal of Hospital Infection, 2012. **80**(4): p. 345-347.
13. Modi, A., et al., *Performance analysis of a solar photovoltaic operated domestic refrigerator.* Applied Energy, 2009. **86**(12): p. 2583-2591.
14. Ullah, K.R., et al., *A review of solar thermal refrigeration and cooling methods.* Renewable and Sustainable Energy Reviews, 2013. **24**: p. 499-513.
15. Govorov, A.O. and H.H. Richardson, *Generating heat with metal nanoparticles.* Nano Today, 2007. **2**(1): p. 30-38.
16. Menbari, A., A.A. Alemrajabi, and A. Rezaei, *Heat transfer analysis and the effect of CuO/Water nanofluid on direct absorption concentrating solar collector.* Applied Thermal Engineering, 2016. **104**: p. 176-183.
17. Otanicar, T.P., et al., *Nanofluid-based direct absorption solar collector.* Journal of Renewable and Sustainable Energy, 2010. **2**(3): p. 033102.
18. Parvin, S., R. Nasrin, and M.A. Alim, *Heat transfer and entropy generation through nanofluid filled direct absorption solar collector.* International Journal of Heat and Mass Transfer, 2014. **71**: p. 386-395.
19. Vijayaraghavan, S., S. Ganapathisubbu, and C. Santosh Kumar, *Performance analysis of a spectrally selective concentrating direct absorption collector.* Solar Energy, 2013. **97**: p. 418-425.
20. Tian, Y. and C.Y. Zhao, *A review of solar collectors and thermal energy storage in solar thermal applications.* Applied Energy, 2013. **104**: p. 538-553.
21. Kalogirou, S.A., *Solar thermal collectors and applications.* Progress in Energy and Combustion Science, 2004. **30**(3): p. 231-295.
22. Liu, J., et al., *A combined numerical and experimental study on graphene/ionic liquid nanofluid based direct absorption solar collector.* Solar Energy Materials and Solar Cells, 2015. **136**: p. 177-186.

Formatted: Font color: Blue

Formatted: Font color: Blue

23. Wijeysundera, N.E. and V. Thevendran, *A two-dimensional heat transfer analysis of the thermal-trap collector.* Solar Energy, 1988. **40**(2): p. 127-133.
24. Arai, N., Y. Itaya, and M. Hasatani, *Development of a "volume heat-trap" type solar collector using a fine-particle semitransparent liquid suspension (FPSS) as a heat vehicle and heat storage medium Unsteady, one-dimensional heat transfer in a horizontal FPSS layer heated by thermal radiation.* Solar Energy, 1984. **32**(1): p. 49-56.
25. Boriskina, S.V., H. Ghasemi, and G. Chen, *Plasmonic materials for energy: From physics to applications.* Materials Today, 2013. **16**(10): p. 375-386.
26. Lenert, A. and E.N. Wang, *Optimization of nanofluid volumetric receivers for solar thermal energy conversion.* Solar Energy, 2012. **86**(1): p. 253-265.
27. Chen, M., et al., *An experimental investigation on sunlight absorption characteristics of silver nanofluids.* Solar Energy, 2015. **115**: p. 85-94.
28. Bandarra Filho, E.P., et al., *Experimental investigation of a silver nanoparticle-based direct absorption solar thermal system.* Energy Conversion and Management, 2014. **84**: p. 261-267.
29. Chen, M., et al., *Investigating the collector efficiency of silver nanofluids based direct absorption solar collectors.* Applied Energy, 2016. **181**: p. 65-74.
30. Eustis, S. and M.A. El-Sayed, *Why gold nanoparticles are more precious than pretty gold: Noble metal surface plasmon resonance and its enhancement of the radiative and nonradiative properties of nanocrystals of different shapes.* Chemical Society Reviews, 2006. **35**(3): p. 209-217.
31. Pérez-Juste, J., et al., *Gold nanorods: Synthesis, characterization and applications.* Coordination Chemistry Reviews, 2005. **249**(17–18): p. 1870-1901.
32. Zhang, H., et al., *Photothermal conversion characteristics of gold nanoparticle dispersions.* Solar Energy, 2014. **100**: p. 141-147.
33. Rahman, M.M., et al., *Effect of solid volume fraction and tilt angle in a quarter circular solar thermal collectors filled with CNT–water nanofluid.* International Communications in Heat and Mass Transfer, 2014. **57**: p. 79-90.
34. Said, Z., et al., *Analyses of exergy efficiency and pumping power for a conventional flat plate solar collector using SWCNTs based nanofluid.* Energy and Buildings, 2014. **78**: p. 1-9.
35. Yousefi, T., et al., *An experimental investigation on the effect of pH variation of MWCNT–H2O nanofluid on the efficiency of a flat-plate solar collector.* Solar Energy, 2012. **86**(2): p. 771-779.
36. He, Q., et al., *Experimental investigation on photothermal properties of nanofluids for direct absorption solar thermal energy systems.* Energy Conversion and Management, 2013. **73**: p. 150-157.
37. Gupta, H.K., G.D. Agrawal, and J. Mathur, *An experimental investigation of a low temperature Al2O3-H2O nanofluid based direct absorption solar collector.* Solar Energy, 2015. **118**: p. 390-396.
38. Yousefi, T., et al., *An experimental investigation on the effect of Al2O3–H2O nanofluid on the efficiency of flat-plate solar collectors.* Renewable Energy, 2012. **39**(1): p. 293-298.
39. Said, Z., et al., *Performance enhancement of a Flat Plate Solar collector using Titanium dioxide nanofluid and Polyethylene Glycol dispersant.* Journal of Cleaner Production, 2015. **92**: p. 343-353.
40. Ghasemi, H., et al., *Solar steam generation by heat localization.* Nat Commun, 2014. **5**.
41. Jin, H., et al., *Steam generation in a nanoparticle-based solar receiver.* Nano Energy.
42. Neumann, O., et al., *Compact solar autoclave based on steam generation using broadband light-harvesting nanoparticles.* Proc Natl Acad Sci U S A, 2013. **110**(29): p. 11677-81.
43. Ni, G., et al., *Volumetric solar heating of nanofluids for direct vapor generation.* Nano Energy, 2015. **17**: p. 290-301.
44. Neumann, O., et al., *Solar vapor generation enabled by nanoparticles.* ACS Nano, 2013. **7**(1): p. 42-9.

Formatted: Font color: Blue

45. Fang, Z., et al., *Evolution of Light-Induced Vapor Generation at a Liquid-Immersed Metallic Nanoparticle.* Nano Letters, 2013. **13**(4): p. 1736-1742.
46. Lukianova-Hleb, E., et al., *Plasmonic nanobubbles as transient vapor nanobubbles generated around plasmonic nanoparticles.* ACS Nano, 2010. **4**(4): p. 2109-2123.
47. Jin, H., et al., *Steam generation in a nanoparticle-based solar receiver.* Nano Energy, 2016. **28**: p. 397-406.
48. Jin, H., et al., *Photothermal conversion efficiency of nanofluids: An experimental and numerical study.* Solar Energy, 2016. **139**: p. 278-289.
49. Baffou, G., et al., *Super-heating and micro-bubble generation around plasmonic nanoparticles under cw illumination.* Journal of Physical Chemistry C, 2014. **118**(9): p. 4890-4898.
50. Carlson, M.T., A.J. Green, and H.H. Richardson, *Superheating water by CW excitation of gold nanodots.* Nano Letters, 2012. **12**(3): p. 1534-1537.
51. Lombard, J., T. Biben, and S. Merabia, *Kinetics of Nanobubble Generation Around Overheated Nanoparticles.* Physical Review Letters, 2014. **112**(10): p. 105701.
52. Hogan, N.J., et al., *Nanoparticles heat through light localization.* Nano Letters, 2014. **14**(8): p. 4640-4645.
53. Zhang, H., et al., *Dependence of Photothermal Conversion Characteristics on Different Nanoparticle Dispersions.* Journal of Nanoscience and Nanotechnology, 2015. **15**(4): p. 3055-3060.
54. Chen, H.-J. and D. Wen, *Ultrasonic-aided fabrication of gold nanofluids.* Nanoscale Research Letters, 2011. **6**(1): p. 198.
55. Xu, J., et al., *Design, Construction, and Characterization of an Adjustable 70 kW High-Flux Solar Simulator.* Journal of Solar Energy Engineering, 2016. **138**(4): p. 041010-041010.

List of Figures

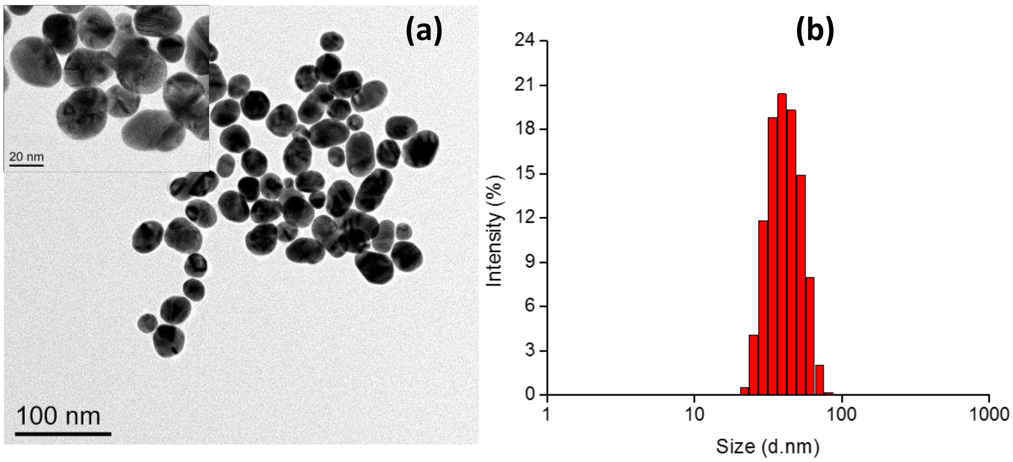

Fig. 1 Characterization of the synthesized gold nanoparticles, (a) TEM image of the gold nanoparticles showing a good suspension and size variation and (b) hydrodynamic size distribution of the gold nanoparticles measured by DLS.

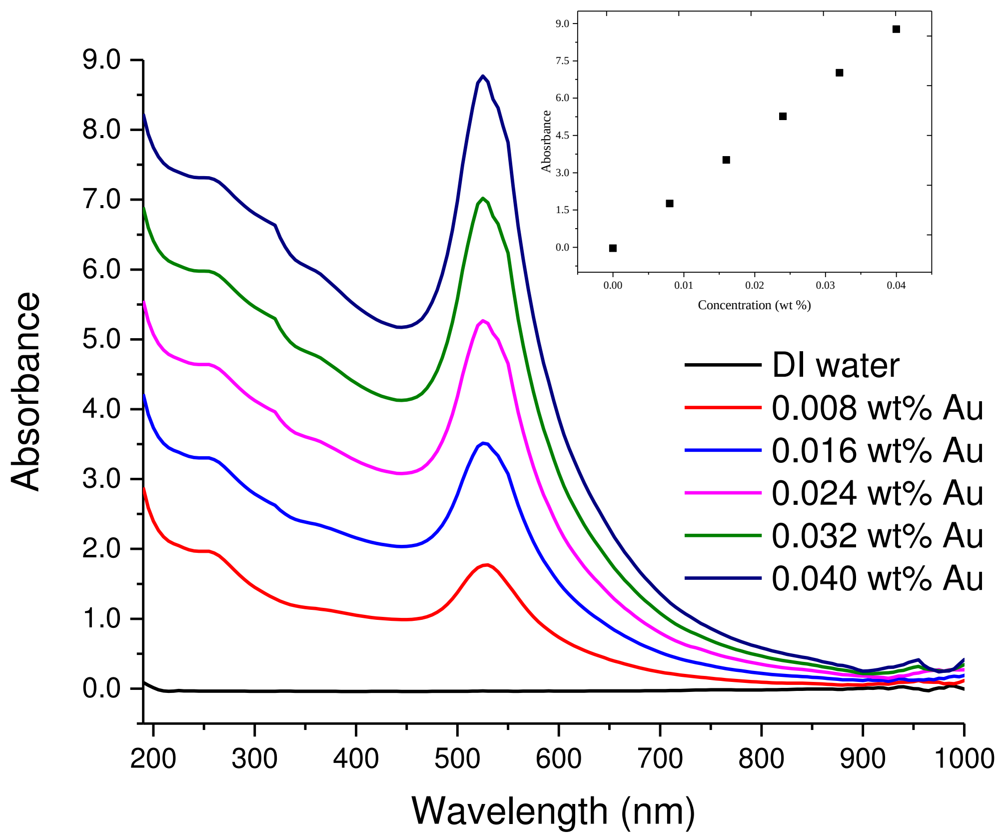

Fig. 2 Optical absorbance spectra of the gold nanofluids at various weight concentrations showing the absorbance peak at plasmonic resonance wavelength of 525nm. The inset shows a linear relationship of the absorbance peak with the concentration.

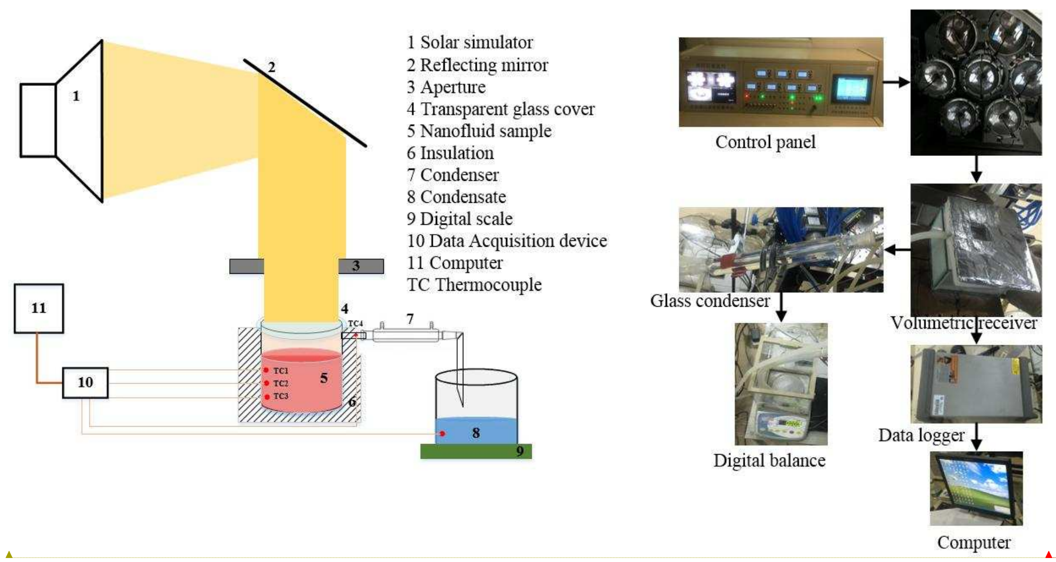

Fig. 33 Schematic of the experimental setup highlighting the major components.

Formatted: Font color: Blue

Formatted: Font color: Blue

Formatted: Font color: Blue

Formatted: Font color: Blue

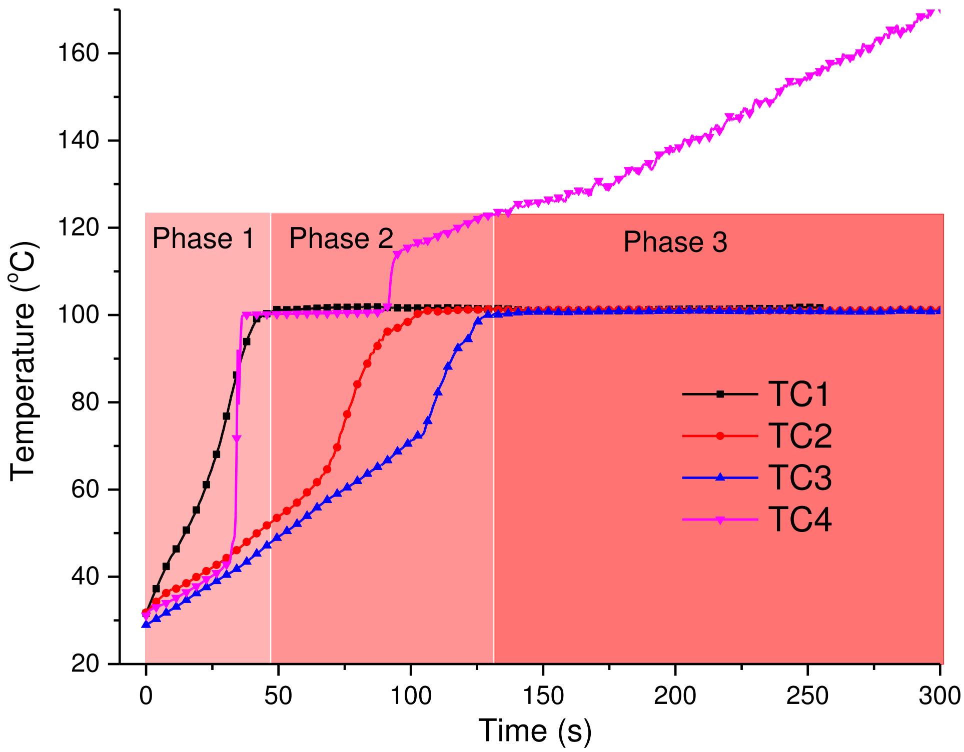

Fig. 4 Temperature distribution during the 5 min illumination of 0.016 wt% Au nanofluid sample where phase 1 shows the surface heating, phase 2 is the bulk fluid heating and phase 3 shows the saturated boiling of the sample. Here TC1, TC2 and TC3 are the temperatures of the thermocouples 1, 2 and 3 and TC4 is the temperature of the steam.

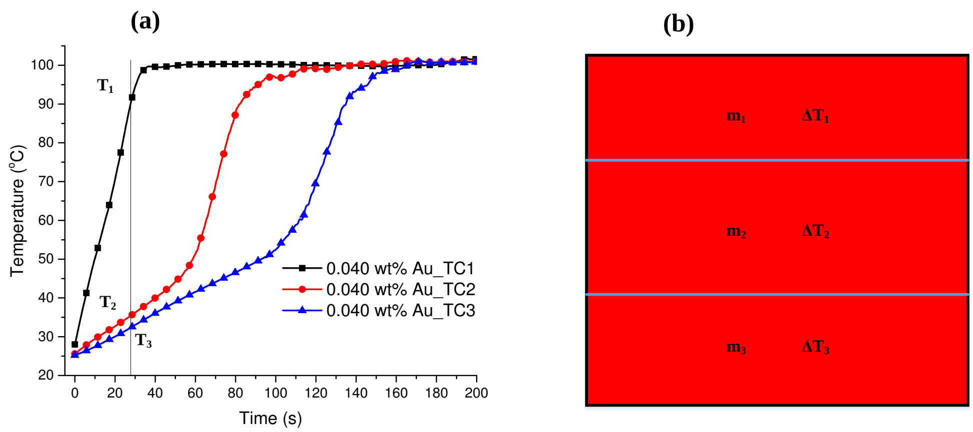

Fig. 5 (a) Variation of temperature along the depth of the 0.040 wt% Au nanofluid sample where T_1, T_2 and T_3 show the reading of thermocouples TC1, TC2 and TC3 respectively and (b) division of fluid volume into different levels as per the temperature distribution during fluid heating.

Field Code Changed

Formatted: Font color: Blue

Formatted: Font color: Blue

Formatted: Font color: Blue

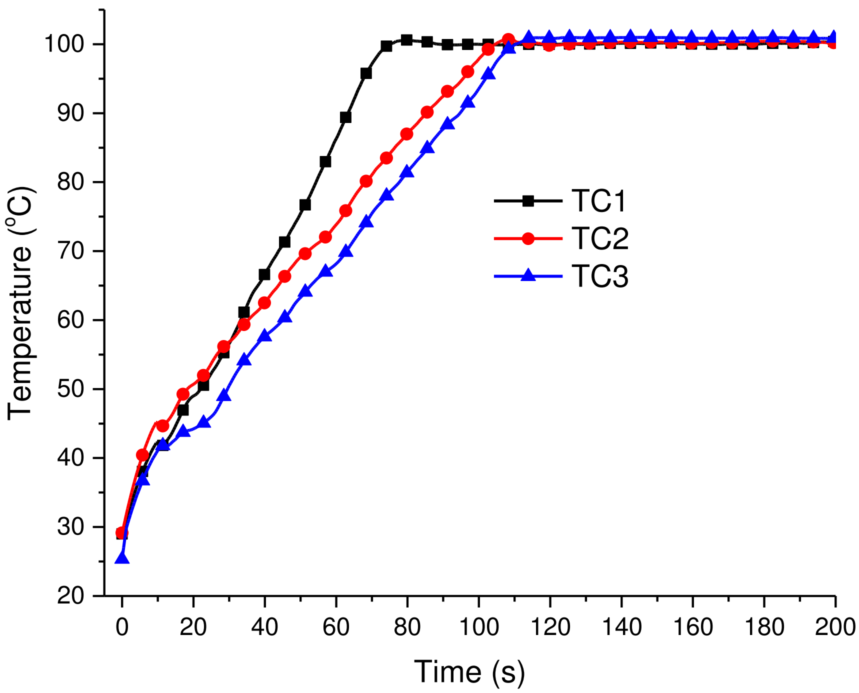

Fig. 6 Temperature distribution of the deionized water sample during the volumetric heating under the illumination of 280 Suns.

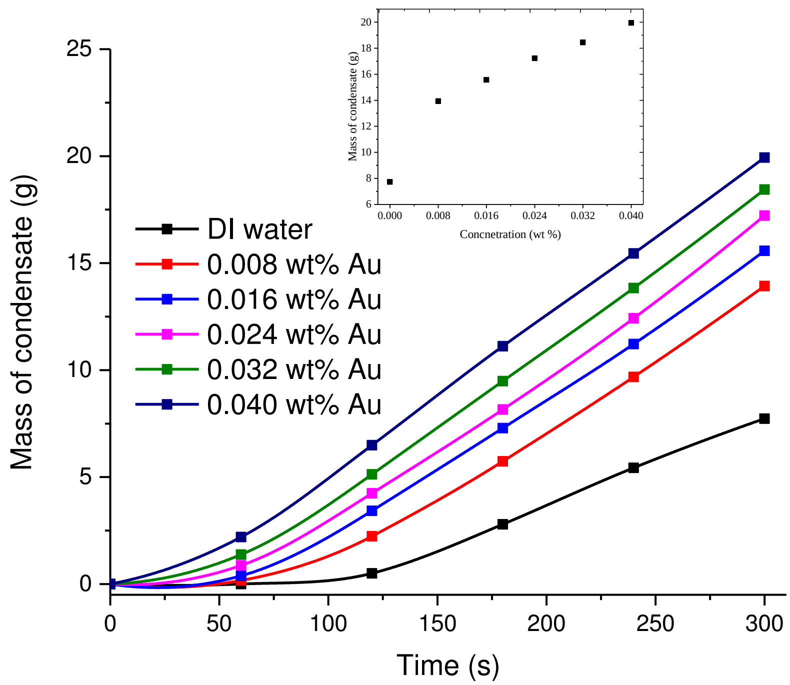

Fig. 7 Mass variation of the condensed vapors at different nanoparticle concentrations as the sample is illuminated with a radiation flux of 280 Suns for a period of 5 min.

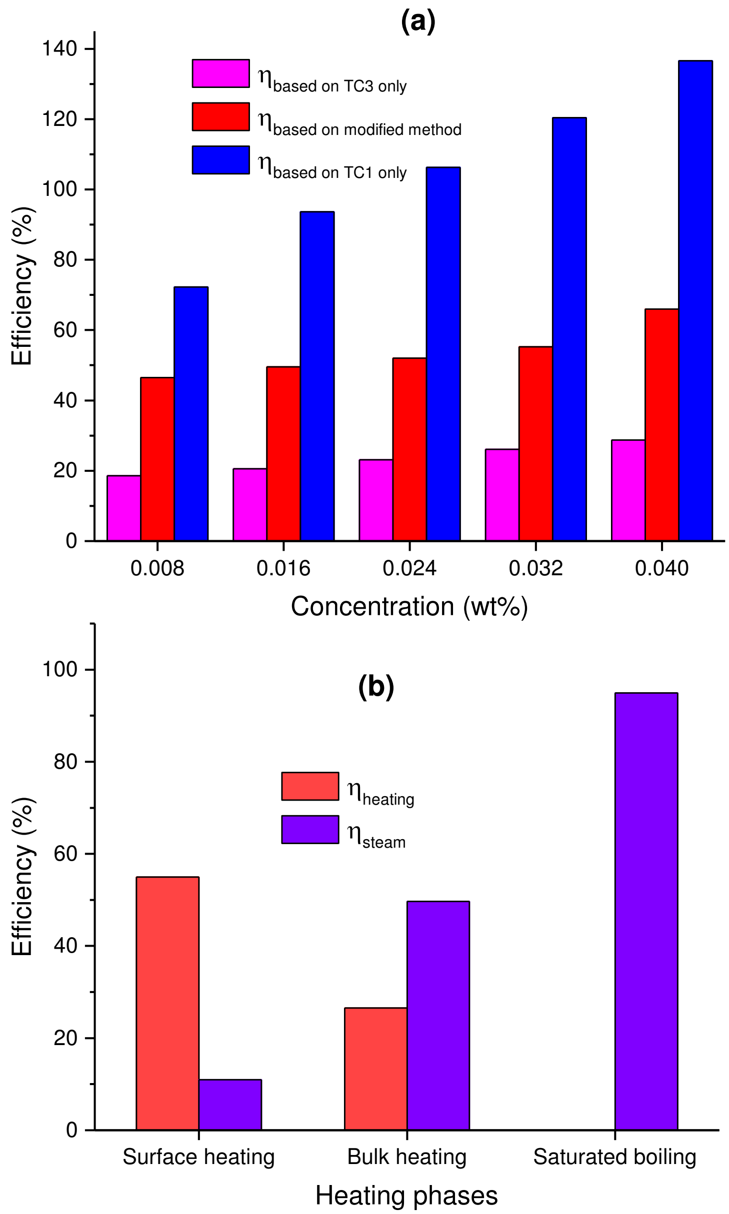

Fig. 8 (a) Efficiency (including latent heat) based on individual thermocouple and modified method at various nanoparticle concentrations during the phase 1 only and (b) Efficiency of sensible heating and steam generation during the three heating phases of 0.040% gold nanofluid sample where $\eta_{heating}$ is based on modified method

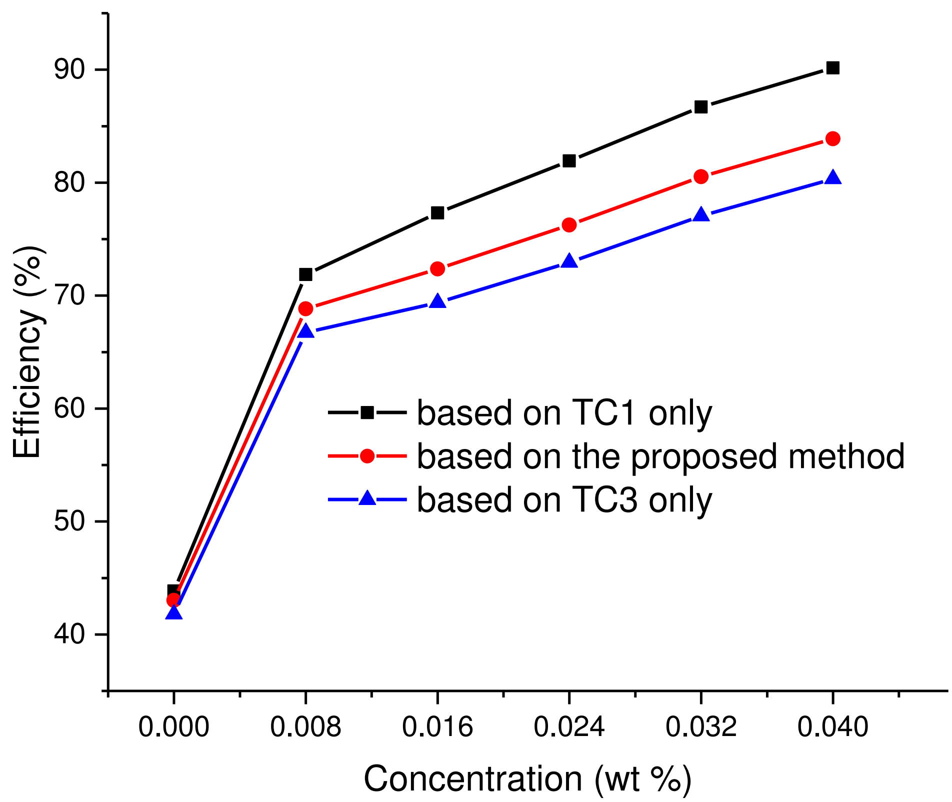

Fig. 9 Photothermal conversion efficiency (η_{PTC}) based on three methods at various nanoparticle concentrations over an irradiation time of 5 min.

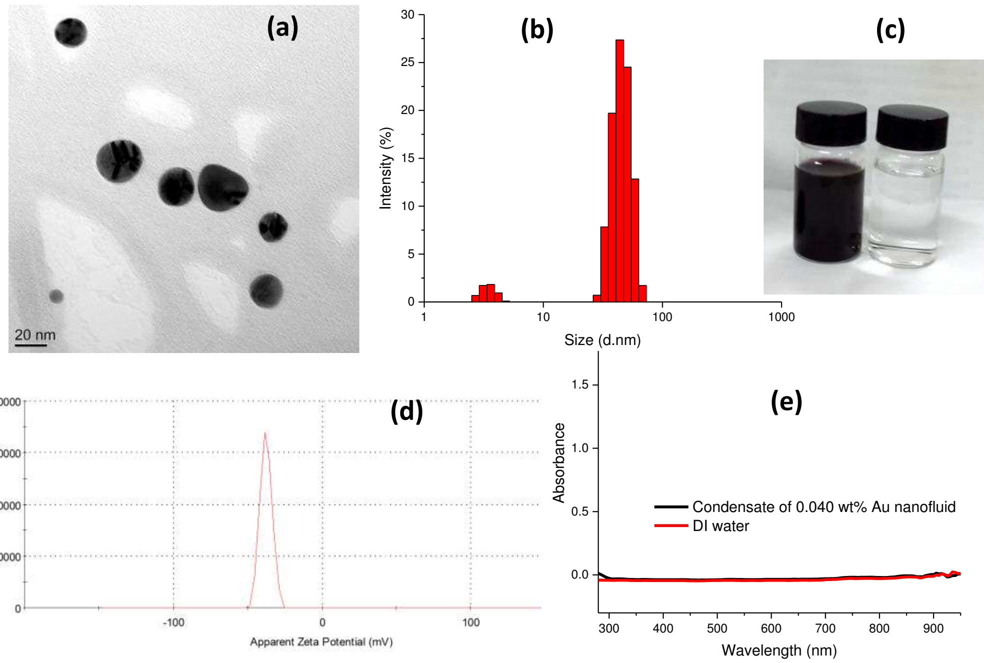

Fig. 10 Characterization of nanoparticles after the steam generation experiment. (a) TEM micrograph, (b) particle size distribution, (c) well stable concentrated left over gold nanosuspension (right) after evaporation and clear condensate (left), (d) zeta potential graph and (e) optical absorbance spectrum of the condensate showing the absence of nanoparticles as can also be seen from the clear color of condensate in (c).

UNIVERSITY OF LEEDS

Professor Dongsheng Wen
(DPhil, CEng, CSci FRSC, FEI, FIoN)
Chair in Petroleum Engineering
School of Process Environment Materials Engineering
University of Leeds, LS2 9JU, U.K
Email: d.wen@leeds.ac.uk : Tel: 0044-113 3431299

20/03/2017

Professor Jinyue Yan
Editor-in-Chief of Applied Energy

Dear Professor Yan

Re: Volumetric solar heating and steam generation via gold nanofluids

Many thanks for organizing the review of the above paper submitted to *Applied Energy*. The authors are grateful for all the constructive comments from the reviewer and the Editor. Most of the comments were concerned on the presentation of the work. We have addressed all these concerns in the revised version, and supplied a point-by-point reply. In the revised version,

- The originality of the work was further highlighted
- The presentation of the work was improved and many ambiguities were clarified
- A careful proof reading was conducted with many typological and grammatical errors removed, including all those raised by the reviewers.
- Reference was updated with four more relevant ones from Applied Energy

We believe that such effort shall satisfy the high quality demand from *Applied Energy.*

Should you require further information, please do not hesitate to contact me. I look forward to hearing from you soon.

Sincerely yours

Dongsheng Wen